

LEVEL II

23

ADA 083246

AFAPL-TR-79-2120 ✓

**THEORETICAL PERFORMANCE LIMITS FOR NON-STATIC EJECTOR
THRUST AUGMENTORS**

JAMES S. PETTY

January 1980
TECHNICAL REPORT AFAPL-TR-79-2120
Final Report for Period February 1979-September 1979

Approved for Public Release; Distribution Unlimited

AIR FORCE AERO PROPULSION LABORATORY
AIR FORCE WRIGHT AERONAUTICAL LABORATORIES
AIR FORCE SYSTEMS COMMAND
WRIGHT-PATTERSON AIR FORCE BASE, OHIO 45433

DTIC
ELECTE
S APR 22 1980 D
E

DC FILE COPY

80 4 21 087


NOTICE

When Government drawings, specifications, or other data are used for any purpose other than in connection with a definitely related Government procurement operation, the United States Government thereby incurs no responsibility nor any obligation whatsoever; and the fact that the government may have formulated, furnished, or in any way supplied the said drawings, specifications, or other data, is not to be regarded by implication or otherwise as in any manner licensing the holder or any other person or corporation, or conveying any rights or permission to manufacture, use, or sell any patented invention that may in any way be related thereto.


This report has been reviewed by the Information Office (OI) and is releasable to the National Technical Information Service (NTIS). At NTIS, it will be available to the general public, including foreign nations.

This technical report has been reviewed and is approved for publication.


JAMES S. PETTY
Project Engineer


DAVID H. QUICK, Lt Col, USAF
Chief, Components Branch

FOR THE COMMANDER


H. I. BUSH, Deputy Director
Turbine Engine Division

"If your address has changed, if you wish to be removed from our mailing list, or if the addressee is no longer employed by your organization please notify AFWAL/POTC, V-P/AFB, OH 45433 to help us maintain a current mailing list".

Copies of this report should not be returned unless return is required by security considerations, contractual obligations, or notice on a specific document.

SECURITY CLASSIFICATION OF THIS PAGE (When Data Entered)

REPORT DOCUMENTATION PAGE		READ INSTRUCTIONS BEFORE COMPLETING FORM
1. REPORT NUMBER 14 AFAPL-TR-79-2120	2. GOVT ACCESSION NO. AD-A083 JV	3. RECIPIENT'S CATALOG NUMBER 9
4. TITLE (and Subtitle) THEORETICAL PERFORMANCE LIMITS FOR NON-STATIC EJECTOR THRUST AUGMENTORS		5. TYPE OF REPORT & PERIOD COVERED Final Report February - September 1979 PERFORMING ORG. REPORT NUMBER
7. AUTHOR(s) James S. Petty		8. CONTRACT OR GRANT NUMBER(s) 101340-1 121461
9. PERFORMING ORGANIZATION NAME AND ADDRESS Air Force Aero Propulsion Laboratory (POTC) Air Force Wright Aeronautical Laboratories (AFSC) Wright-Patterson Air Force Base, Ohio 45433		10. PROGRAM ELEMENT, PROJECT, TASK AREA & WORK UNIT NUMBERS Program Element 62203F, Project 3066, Task 306606, Work Unit 30660602
11. CONTROLLING OFFICE NAME AND ADDRESS		12. REPORT DATE 11 January 1980
14. MONITORING AGENCY NAME & ADDRESS (if different from Controlling Office)		13. NUMBER OF PAGES 46
		15. SECURITY CLASS. (of this report) Unclassified
		15a. DECLASSIFICATION DOWNGRADING SCHEDULE
16. DISTRIBUTION STATEMENT (of this Report) Approved for public release; distribution unlimited.		
17. DISTRIBUTION STATEMENT (of the abstract entered in Block 20, if different from Report)		
18. SUPPLEMENTARY NOTES		
19. KEY WORDS (Continue on reverse side if necessary and identify by block number) Ejectors Thrust Augmentation Cycle Analysis		
20. ABSTRACT (Continue on reverse side if necessary and identify by block number) An analytical study was performed to determine the theoretical limits on the pre- formance of non-static ejector thrust augmentors. Idealizing assumptions were made, such as inviscid compressible working fluids, isentropic flows in inlets, diffusers, nozzles and ducts, constant pressure mixing, and thermally and calo- rically perfect fluids. By ignoring details of the primary flow "pump," the performance of ejector augmentors was found in terms of three parameters (the secondary/primary mass flow ratio, a pressure parameter and a temperature para- meter) in a form which was not an explicit function of the flight Mach number.		

DD FORM 1 JAN 73 1473 EDITION OF 1 NOV 65 IS OBSOLETE

SECURITY CLASSIFICATION OF THIS PAGE (When Data Entered)

011570

3012

It was also shown that multi-stage ejectors offered no performance improvement over ideal single-stage ejectors. Two primary "pump" devices, a turbine engine gas generator and an isentropic compressor, were considered. With them, the Mach number dependent behavior of ideal ejectors was determined. As a result of this study, the following conclusions were drawn: 1) The performance of ideal ejector is severely degraded by increasing the primary fluid temperature, 2) The performance of ideal ejectors is degraded faster than that of ideal turbofans as the flight Mach number is increased, 3) Neither the turbine engine nor the isentropic compressor is a suitable "pump" for ideal ejectors, except at very low Mach numbers, and 4) Ejector augmentors should be most useful for low flight speed applications; e.g., V/STOL.

Accession For	
NTIS Global	<input checked="checked" type="checkbox"/>
DDC TAB	<input type="checkbox"/>
Unannounced	<input type="checkbox"/>
Justification	<input type="checkbox"/>
By _____	
Distribution/ _____	
Availability Codes	
Dist	Avail and/or special
A	

FOREWORD

The study reported herein was undertaken as the result of several conversations with Dr Hans J. P. von Ohain, then Chief Scientist of the Air Force Aero Propulsion Laboratory.

The effort was conducted in-house in the Air Force Aero Propulsion Laboratory, Air Force Systems Command, Wright-Patterson AFB, Ohio, under Project 3066, Task 06, Work Unit 02 by Dr James S. Petty (AFWAL/POTC) during the period February 1979-September 1979. The author submitted the report in November 1979.

The author wishes to express his gratitude to Dr von Ohain and to Drs Kervyn D. Mach (AFWAL/POTC) and K. S. Nagaraga (AFWAL/FIMM) for their comments and suggestions. Special appreciation is due to Mrs Carla Morter for typing this report.

PRECEDING PAGE BLANK-NOT FILMED

TABLE OF CONTENTS

SECTION		PAGE
I	INTRODUCTION	1
	1. Background	1
	2. Assumptions	2
	3. Description of an Ideal Ejector Augmentor	2
II	IDEAL CYCLE ANALYSES	5
	1. Equation of State	5
	2. Ejector Augmentor (Single Stage)	6
	3. Ejector Augmentor (Multi-Stage)	9
	4. Mixed-Flow Turbofan	12
	5. The Isentropic Compressor	14
	6. Core Turbine Engine Gas Generator	15
III	DISCUSSION	17
	1. An Ideal Thrust Augmentor	17
	2. Comparison of Entropies	17
	3. Ideal Performance Contour Maps	18
	4. Mach Number Dependence of Limits on Performance	20
	5. Ejector Augmentor with an Isentropic Compressor	21
	6. Ejector Augmentor with Turbine Engine Gas Generator	22
IV	CONCLUSIONS	23
	APPENDIX - Maximum Thrust Augmentation	25
	ILLUSTRATIONS	28
	REFERENCES	46

LIST OF ILLUSTRATIONS

FIGURE		PAGE
1	Ejector Thrust Augmentor	28
	a. Schematic Drawing	
	b. T-S Diagram	
2	Schematic of One Stage of a Multi-stage Ejector Augmentor	29
3	Turbofan Engine	30
	a. Schematic Drawing	
	b. T-S Diagram	
4	T-S Diagram for an Ideal Turbine Engine Gas Generator	31
5	Performance Maps for Ideal Ejector Augmentors	32
	a. Mass Flow Ratio = 1	32
	b. Mass Flow Ratio = 2	33
	c. Mass Flow Ratio = 5	34
	d. Mass Flow Ratio = 10	35
	e. Mass Flow Ratio = 20	36
6	Performance Maps for Ideal Turbofans	37
	a. Mass Flow Ratio = 1	37
	b. Mass Flow Ratio = 2	38
	c. Mass Flow Ratio = 5	39
7	Attainable Regions of Performance Maps for Various Mach Numbers	40
8	Isentropic Compressor Curves for Various Mach Numbers	41
9	Performance Maps for Ideal Ejectors with Turbine Engine Cores	42
	a. Mach Number = 0.2	42
	b. Mach Number = 0.7	43
	c. Mach Number = 1.4	44
10	Mapping of the Turbine Engine Region of Figure 8 for Various Mach numbers	45

LIST OF SYMBOLS

<u>SYMBOL</u>	<u>QUANTITY</u>
C_p	specific heat at constant pressure
f	specific thrust, $F/\dot{m}_p u_\infty$
F	thrust
h	enthalpy, $C_p T$
\bar{h}	nondimensional temperature or enthalpy, T/T_∞
M	Mach number
\dot{m}_p	primary or core mass flow rate
p	pressure
s	entropy
T	absolute temperature
u	velocity
\bar{u}	nondimensional velocity, $u/h_\infty^{1/2}$
α	turbine engine compressor parameter (Page 15)
β	secondary/primary mass flow ratio (bypass ratio)
γ	ratio of specific heats
$\Delta \bar{h}_c$	nondimensional combustor temperature rise
ΔT_c	combustor temperature rise
Δs	difference of entropy variables
ζ	mixing pressure parameter, $(1 - \frac{1}{\pi_m}) / (1 - \frac{1}{\pi_{ts}})$
μ	temperature parameter, $(T_{ts}/T_{tp})^{1/2}$
ν	pressure parameter, $(1 - \frac{1}{\pi_{ts}})^{1/2} / (1 - \frac{1}{\pi_{tp}})^{1/2}$
ξ	mass flow fraction (Page 9)
π	nondimensional pressure variable, $(p/p_\infty)^{\frac{\gamma-1}{\gamma}}$
ϕ	augmentation ratio, $f/f_{\beta=0}$

SUBSCRIPTS

a	at ambient pressure
c	compressor exit condition (except in $\Delta \bar{h}_c$ and ΔT_c)
e	in the exhaust
ej	ejector

LIST OF SYMBOLS (concluded)

<u>SYMBOL</u>	<u>QUANTITY</u>
SUBSCRIPTS	
isen	isentropic compressor
m	at or in the mixer
p	primary (core) flow (except in C_p)
s	secondary (bypass) flow
t	first subscript - stagnation (total) condition second subscript - at the turbine inlet
tf	turbofan
∞	ambient static (freestream) condition
SUPERSSCRIPTS	
*	optimum
(i), (n), (N)	stage number (multi-stage ejector)

SECTION I

INTRODUCTION

1. BACKGROUND

The idea of using ejector devices to obtain thrust augmentation for gas turbine engines is not new. However, it has received increased attention during the past decade or so, due in part to the significant advances which have been realized in the design and performance of static (stationary) ejector augmentors.

In his 1966 paper⁽¹⁾, Heiser reported on an analytic study of thrust augmentation, in which he used a few basic assumptions and the conservation laws. His analysis of ejector augmentors was limited to static devices with constant area mixers and incompressible flows. He showed that, except for small bypass ratios (secondary/primary mass flow ratio), the thrust augmentation ratios attainable by ejectors were considerably less than those of ideal thrust augmentors, and were limited to values of less than two.

In an earlier note⁽²⁾, Knox briefly discussed the optimum performance of the nonstationary, constant pressure mixing ejector augmentor. His results indicate that potential performance is possible which is considerably better than Heiser's predictions. The only flaw we find with Knox's results is that he did not consider the primary (high pressure) fluid to have been collected from the atmosphere, and hence, did not include its contribution to the ram drag.

In this study, we have sought to ascertain the theoretical limits of performance for nonstationary ejector augmentors, compared with those of turbofan engines. To do this, we have essentially re-derived and extended Knox's results by also examining turbofans, multistage ejectors and various "pump" devices.

Using an aerothermodynamic cycle analysis, the performance of the ideal ejector augmentor is examined without making any assumptions about the primary "pump" device which supplies the high pressure working fluid. Both single and multiple stage ejectors are considered. The ideal mixed-flow turbofan is also analyzed for comparison. Finally, the influences of two "pump" devices - an isentropic compressor and a turbine engine gas generator are addressed.

2. ASSUMPTIONS

In order to make our analysis ideal (and tractable), we have made a number of assumptions about the working fluids and the thrust augmenting devices:

- o Perfect gases - Both the primary and secondary gasses are calorically and thermally perfect, and both have the same value for γ , the ratio of the specific heats.
- o Inviscid, compressible flow - Both the primary and secondary flows are inviscid and compressible.
- o Uniform flows - All flow fields are uniform in the direction normal to the flow direction, e.g., no transverse pressure gradients.
- o Isentropic or adiabatic processes - All flows in inlets, diffusers, nozzles, ducts, compressors and turbines are isentropic; i.e., no shock losses, or skin friction or heat transfer losses. All mixing processes are adiabatic; i.e., no skin friction or heat transfer losses.
- o Constant pressure mixing - All mixing processes occur at constant pressure.

These assumptions generally produce performance estimates for thrust augmentation devices which are greater than those

physically attainable, and thus, can serve as optimistic upper bounds for performance. The possible exception is the assumption of perfect gases. We will not, however, address the effects of thermal and caloric imperfections on ejector performance.

3. DESCRIPTION OF AN IDEAL EJECTOR AUGMENTOR

Figure 1* is a schematic sketch of an ideal ejector augmentor with a temperature-entropy (T-S) diagram for the ejector cycle assuming complete mixing of the primary and secondary flows. The operation of the ejector augmentor may be described as follows:

Ambient air is captured by the inlet and isentropically diffused to stagnation conditions. On the T-S diagram, this is represented by the vertical line from $(p_{\infty}, T_{\infty}, s_{\infty})$ to $(p_{ts}, T_{ts}, s_{\infty})$.

A portion of this diffused flow is then pumped by some means to the primary reservoir conditions (p_{tp}, T_{tp}, s_p) . The remainder of the captured flow forms the secondary, or bypass, flow. The mass fractions of the captured air in the primary and secondary flows are $\frac{1}{1+\beta}$ and $\frac{\beta}{1+\beta}$, where β is the secondary/primary mass flow ratio (bypass ratio).

The primary and secondary flows are expanded through nozzles to some mixing pressure p_m . This is represented on the T-S diagram by the vertical lines from the primary and secondary reservoir conditions down to the mixing pressure isobar.

The two flows are completely mixed adiabatically at constant pressure, as represented by the lines along the p_m isobar to the mixed flow isentrope.

*All illustrations appear at the end of this report.

The mixed flow is then expanded or diffused, as required, through the exhaust nozzle to ambient pressure. We consider this to be a two-step process; the first step being the isentropic recovery of the flow to stagnation conditions (p_{tm} , T_{tm} , s_m), and the second step being the isentropic expansion of the stagnant flow to ambient pressure. This is represented on the diagram by moving vertically along the mixed flow isentrope upward to the mixed flow total temperature isotherm and then downward to the ambient pressure isobar.

SECTION II

IDEAL CYCLE ANALSES

1. EQUATION OF STATE

For convenience in the following analyses, we will use a modified form of the equation of state with nondimensional enthalpy, entropy and pressure variables. Since the gas is assumed to be thermally and calorically perfect, the temperature, pressure and entropy are related by the equation.⁽³⁾

$$T/T_{\infty} = (p/p_{\infty})^{\frac{\gamma-1}{\gamma}} e^{(s-s_{\infty})/C_p}$$

where $()_{\infty}$ refers to ambient conditions. Defining the nondimensional variables

$$\begin{aligned}\bar{h} &= T/T_{\infty} \\ \pi &= (p/p_{\infty})^{\frac{\gamma-1}{\gamma}} \\ \sigma &= e^{(s-s_{\infty})/C_p}\end{aligned}$$

the equation of state which we use is obtained:

$$\bar{h} = \pi \sigma$$

Since $h/h_{\infty} = T/T_{\infty}$ for a calorically perfect gas, \bar{h} , is also the nondimensional specific enthalpy. These variables have the minor advantage that constant pressure, temperature and entropy curves in a T-S diagram are all straight lines on the equivalent \bar{h} -s diagram.

In the remainder of this Section, when we refer to temperature (or enthalpy), entropy or pressure, we mean the equivalent nondimensional variable, \bar{h} , σ or π , unless otherwise specified.

2. EJECTOR AUGMENTOR (SINGLE STAGE)

The analysis of the single stage ejector augmentor cycle shown in Figure 1 is relatively straightforward. Given the total conditions (\bar{h}_{tp} , π_{tp} , \bar{h}_{ts} , π_{ts}) of the primary and secondary flows and the mixing pressure π_m , the primary and secondary static enthalpies (\bar{h}_{mp} , \bar{h}_{ms}) at the entrance to the mixer are determined, and hence, the primary and secondary mixing velocities:

$$\bar{h}_{mp} = \bar{h}_{tp} \pi_m / \pi_{tp} \quad (1)$$

$$\tilde{u}_p^2 = 2(\bar{h}_{tp} - \bar{h}_{mp}) \quad (2)$$

etc., where $\tilde{u} = u/h_\infty^{1/2}$ is a nondimensional velocity. The mixing process itself is described globally by the conservation of energy and momentum. Since the mixing is assumed to be adiabatic and inviscid, the conservation of energy gives

$$(1 + \beta) \bar{h}_{tm} = \bar{h}_{tp} + \beta \bar{h}_{ts} \quad (3)$$

where β is the secondary/primary mass flow ratio. Under the assumption of constant pressure mixing and inviscid flow, the pressure and viscous terms drop out of the momentum equation, and the conservation of momentum gives simply

$$(1 + \beta) \tilde{u} = \tilde{u}_p + \beta \tilde{u}_s \quad (4)$$

At the end of the mixing zone, the static enthalpy and entropy are given by

$$\bar{h}_m = \bar{h}_{tm} - \frac{1}{2} \tilde{u}_m^2 \quad (5)$$

$$\sigma_m = \bar{h}_m / \pi_m \quad (6)$$

Finally, the expansion of the mixed flow through the exhaust nozzle to ambient conditions gives the exhaust velocity

$$\begin{aligned}
\tilde{u}_e &= \sqrt{2} (\tilde{h}_{tm} - \tilde{h}_{am})^{\frac{1}{2}} \\
&= \sqrt{2} (\tilde{h}_{tm} - \pi_\infty \sigma_m)^{\frac{1}{2}} \\
&= \sqrt{2} (\tilde{h}_{tm} - \sigma_m)^{\frac{1}{2}} \quad (7)
\end{aligned}$$

(the latter because $\pi_\infty = 1$), and the specific thrust ($f = F/\dot{m}_p u_\infty$)

$$f = (1 + \beta) (\tilde{u}_e / \tilde{u}_\infty - 1) \quad (8)$$

In this equation for the specific thrust, we assume that both the primary and secondary fluids consist of captured ambient air, and hence, contribute to the ram drag.

The solution of these equations is relatively straightforward. However, we are not particularly interested in the solution for arbitrary mixing pressures, but only in the solution at the mixing pressures which maximize the specific thrust.

As can be seen from examination of Equations (7) and (8), the specific thrust is maximized by minimizing the entropy σ_m of the mixed flow. With a little algebraic manipulation of Equations (1) through (6), the entropy of the mixed flow can be expressed as

$$\sigma_m = \frac{\tilde{h}_{tm}}{\pi_m} - \frac{1}{(1 + \beta)^2} \left[\left(\frac{\tilde{h}_{tp}}{\pi_m} - \sigma_p \right)^{\frac{1}{2}} + \beta \left(\frac{\tilde{h}_{ts}}{\pi_m} - \sigma_s \right)^{\frac{1}{2}} \right]^2 \quad (9)$$

Taking the derivative of this equation with respect to π_m , setting it equal to zero and solving for π_m , we obtain the following solutions for the optimum mixing pressure:

$$\pi_m^* = (\tilde{h}_{tp} - \tilde{h}_{ts}) / \left(\frac{\tilde{h}_{tp}}{\pi_{ts}} - \frac{\tilde{h}_{ts}}{\pi_{tp}} \right), \quad \frac{\tilde{h}_{tp} - \tilde{h}_{ts}}{\sigma_p - \sigma_s} \quad (10)$$

Examination shows that the first solution has the minimum entropy if $\tilde{h}_{tp} \geq \tilde{h}_{ts}$ and $\pi_{tp} \geq \pi_{ts}$, and the second solution has the minimum entropy if $\tilde{h}_{tp} \leq \tilde{h}_{ts}$ and $\pi_{tp} \geq \pi_{ts}$. We will not

consider the second solution further, because $\bar{h}_{tp} > \bar{h}_{ts}$ for ejector thrust augmentors for gas turbine engines. Note that the optimum mixing pressure π_m^* is independent of the mass flow ratio β . By substituting the first solution of Equation (10) into Equation (9), the minimum mixed flow entropy is found to be

$$\sigma_m^* = \frac{1}{(1 + \beta)^2} (\bar{h}_{tp} + \beta \bar{h}_{ts}) \left(\frac{1}{\pi_{tp}} + \beta \frac{1}{\pi_{ts}} \right) \quad (11)$$

and the maximum exhaust velocity

$$\tilde{u}_e^* = \frac{\sqrt{2}}{1 + \beta} (\bar{h}_{tp} + \beta \bar{h}_{ts})^{1/2} \left(\left[1 - \frac{1}{\pi_{tp}} \right] + \beta \left[1 - \frac{1}{\pi_{ts}} \right] \right)^{1/2} \quad (12)$$

We now define two parameters; a "temperature" parameter

$$\mu = (\bar{h}_{ts}/\bar{h}_{tp})^{1/2} \quad (13)$$

and a "pressure" parameter

$$\nu = \left(\frac{1 - \frac{1}{\pi_{ts}}}{1 - \frac{1}{\pi_{tp}}} \right)^{1/2} \quad (14)$$

Using these parameters we may rewrite Equation (12) as

$$\tilde{u}_e^* = [2\bar{h}_{ts} (1 - \frac{1}{\pi_{ts}})]^{1/2} \frac{1}{1 + \beta} \left(\frac{1}{\mu^2} + \beta \right)^{1/2} \left(\frac{1}{\nu^2} + \beta \right)^{1/2} \quad (15)$$

We have assumed that the secondary flow air is obtained by isentropic recovery from ambient conditions, so

$$\begin{aligned} \bar{h}_{ts} = \pi_{ts} &= 1 + \frac{\gamma - 1}{2} M_\infty^2, \quad \sigma_s = 1 \\ \tilde{u}_\infty^2 &= (\gamma - 1) M_\infty^2 = 2(\bar{h}_{ts} - 1) \end{aligned} \quad (16)$$

Substituting from Equations (15) and (16) into Equation (8), the specific thrust is found to be

$$f = \left(\frac{1}{\mu^2} + \beta \right)^{1/2} \left(\frac{1}{\nu^2} + \beta \right)^{1/2} - (1 + \beta) \quad (17)$$

and the augmentation ratio ϕ (defined to be $f/f_{\beta=0}$)

$$\phi = \frac{1}{1 - \mu\nu} [(1 + \beta\mu^2)^{\frac{1}{2}}(1 + \beta\nu^2)^{\frac{1}{2}} - (1 + \beta)\mu\nu] \quad (18)$$

These two equations give the maximum values for the specific thrust and augmentation ratio which can be obtained from an ejector augmentor with complete mixing, given the parameters (β, μ, ν) .

As an aside, if the mixing pressure is not optimum ($\pi_m \neq \pi_m^*$), then the specific thrust is

$$f = \left[\frac{1}{\mu^2\nu^2} + \beta \left(\frac{1}{\mu^2} + 1 \right) \zeta + \beta^2 + 2 \frac{\beta}{\mu} \left(\frac{1}{\nu^2} - \zeta \right)^{\frac{1}{2}} (1 - \zeta)^{\frac{1}{2}} \right]^{\frac{1}{2}} - (1 + \beta)$$

where we have introduced the parameter

$$\zeta = \frac{1 - \frac{1}{\pi_m}}{1 - \frac{1}{\pi_{ts}}}$$

For optimum mixing pressure, $\zeta^* = (1 - \mu^2/\nu^2)/(1 - \mu^2)$. This can be used to evaluate off-optimum ejector augmentor performance.

3. EJECTOR AUGMENTOR (MULTI-STAGE)

The question naturally occurs as to whether or not the performance of the ideal ejector augmentor with a single constant pressure mixing stage can be improved by using an ideal multi-stage mixer in which the secondary flow is introduced incrementally, and in which each stage is optimized.

Consider the incremental mixer stage displayed schematically in Figure 2. As shown, the output of the $(n-1)^{st}$ stage forms the primary flow for the n^{th} stage, and an increment $\xi_s^{(n)}$ of secondary mass flow is added at the n^{th} stage.

Conservation of mass gives, for the n^{th} stage,

$$\xi_p^{(n)} = \xi_m^{(n-1)} \quad (19)$$

$$\xi_m^{(n)} = \xi_p^{(n)} + \xi_s^{(n)} \quad (20)$$

conservation of energy gives

$$\tilde{h}_{tp}^{(n)} = \tilde{h}_{tm}^{(n-1)} \quad (21)$$

$$\tilde{h}_{tm}^{(n)} = (\xi_p^{(n)} \tilde{h}_{tp}^{(n)} + \xi_s^{(n)} \tilde{h}_{ts}^{(n)}) / \xi_m^{(n)} \quad (22)$$

and conservation of momentum, for constant pressure mixing, gives

$$\tilde{u}_m^{(n)} = (\xi_p^{(n)} \tilde{u}_p^{(n)} + \xi_s^{(n)} \tilde{u}_s^{(n)}) / \xi_m^{(n)} \quad (23)$$

The assumption of isentropy between stages gives

$$\sigma_p^{(n)} = \sigma_m^{(n-1)} \quad (24)$$

For a specified mixing pressure $\pi_m^{(n)}$, the mixing velocities of the primary and secondary flows are, respectively,

$$\tilde{u}_p^{(n)} = \sqrt{2} (\tilde{h}_p^{(n)} - \pi_m^{(n)} \sigma_p^{(n)})^{1/2} \quad (25)$$

$$\tilde{u}_s^{(n)} = \sqrt{2} (\tilde{h}_{ts}^{(n)} - \pi_m^{(n)} \sigma_s^{(n)})^{1/2}$$

and the entropy of the mixed flow is

$$\sigma_m^{(n)} = [\tilde{h}_{tm}^{(n)} - \frac{1}{2} (\tilde{u}_m^{(n)})^2] / \pi_m^{(n)} \quad (26)$$

Given that $\xi_p^{(1)} = 1$, Equations (19) and (20) may be immediately solved to give

$$\xi_m^{(n)} = 1 + \sum_{i=1}^n \xi_s^{(i)} \quad (27)$$

and, given that $\bar{h}_{tp}^{(1)} = \bar{h}_{tp}$, Equations (21) and (22) have the solution

$$\bar{h}_{tm}^{(n)} = (\bar{h}_{tp} + \bar{h}_{ts} \sum_{i=1}^n \xi_s^{(i)}) / \xi_m^{(n)} \quad (28)$$

Our analysis of the single stage mixer shows (Equation (10)) that the optimum mixing pressure for the n^{th} stage should be

$$\begin{aligned} \pi_m^{*(n)} &= (\bar{h}_{tp}^{(n)} - \bar{h}_{ts}) / \left(\frac{\bar{h}_{tp}^{(n)}}{\pi_{ts}} - \frac{\bar{h}_{ts}}{\pi^{(n)}} \right) \\ &= (\bar{h}_{tm}^{(n-1)} - \bar{h}_{ts}) / \left(\frac{\bar{h}_{tm}^{(n-1)}}{\pi_{ts}} - \frac{\bar{h}_{ts}}{\bar{h}_{tm}^{(n-1)} \sigma_m^{(n-1)}} \right) \end{aligned}$$

This choice minimizes the entropy increase in each stage. (Which implies that the overall entropy increase of the multi-stage mixer will also be minimized.) With this, Equations (19) through (26) and some algebraic manipulation, the following relation for the entropy of the mixed flow is found:

$$\begin{aligned} \sigma_m^{(n)} &= \frac{\bar{h}_{tm}^{(n)}}{\bar{h}_{tm}^{(n-1)} - \bar{h}_{ts}} \left[(\bar{h}_{tm}^{(n-1)} - \bar{h}_{tm}^{(n)}) \frac{\sigma_s}{\bar{h}_{ts}} + \right. \\ &\quad \left. (\bar{h}_{tm}^{(n)} - \bar{h}_{ts}) \frac{\sigma_m^{(n-1)}}{\bar{h}_{tm}^{(n-1)}} \right] \end{aligned}$$

With the initial condition $\sigma_m^{(0)} = \bar{h}_{tp} / \pi_{tp}$, the solution of this recursion relation may be shown to be

$$\sigma_m^{(n)} = \bar{h}_{tm}^{(n)} \left[\frac{1}{\pi_{tp}} + \frac{1}{\pi_{ts}} \sum_{i=1}^n \xi_s^{(i)} \right] / \xi_m^{(n)} \quad (29)$$

and the optimum mixing pressure $\pi_m^{*(n)}$ for the n^{th} stage is then found to be

$$\pi_m^{*(n)} = (\bar{h}_{tp} - \bar{h}_{ts}) / \left(\frac{\bar{h}_{tp}}{\pi_{ts}} - \frac{\bar{h}_{ts}}{\pi_{tp}} \right) \quad (30)$$

which is a constant, independent of either stage number or mass flow ratio.

If we choose $\xi_s^{(i)}$ such that, for N stages,

$$\beta = \sum_{i=1}^N \xi_s^{(i)}$$

then Equations (27), (28) and (29) give

$$\xi_m^{(N)} = 1 + \beta$$

$$h_{tm}^{(N)} = (h_{tp} + \beta h_{ts}) / (1 + \beta)$$

$$\sigma_m^{(N)} = \frac{1}{(1 + \beta)^2} (h_{tp} + \beta h_{ts}) \left(\frac{1}{\pi_{tp}} + \beta \frac{1}{\pi_{ts}} \right)$$

which results, including Equation (30), are identical to those for a single stage mixer for the same mass flow ratio β . Therefore, ideal incremental staging offers no performance advantage over an ideal single stage.*

4. MIXED-FLOW TURBOFAN

Figure 3 shows a schematic drawing and a T-S diagram for an ideal mixed-flow turbofan. The primary (or core) fluid is isentropically expanded through the turbine to extract power to drive the fan which isentropically compresses the secondary (or bypass) flow. The fan and turbine are matched so that the total pressures of the core and bypass flows are the same at the entry to the mixer. The flows are mixed adiabatically at zero velocity in the mixer and expanded to ambient pressure in the exhaust nozzle.

*This result appears to constitute one step in a proof that the constant pressure mixer is the optimum mixer, i.e., the mixer with the least entropy increase.

The turbofan cycle may be analyzed by using the T-S diagram of Figure 3(b). The work performed by the turbine must equal the work required by the fan, so

$$(\bar{h}_{tp} - \bar{h}_{tpm}) = \beta(\bar{h}_{tsm} - \bar{h}_{ts})$$

The total pressures at the turbine and fan exits must be equal, so

$$\bar{h}_{tsm}/\sigma_s = \bar{h}_{tpm}/\sigma_p = \pi_{tm}$$

Since the flow mixing is adiabatic and at zero velocity, conservation of energy gives

$$\bar{h}_{tpm} + \beta\bar{h}_{tsm} = (1 + \beta)\bar{h}_{tm}$$

The entropy of the mixed flow is given by

$$\sigma_m = \bar{h}_{tm}/\pi_{tm}$$

and the exhaust velocity is

$$\begin{aligned}\bar{u}_e &= \sqrt{2} (\bar{h}_{tm} - \bar{h}_{am})^{1/2} \\ &= \sqrt{2} (\bar{h}_{tm} - \sigma_m)^{1/2}\end{aligned}$$

The solution of these equations is straightforward and will not be detailed here. The results are

$$\begin{aligned}\bar{h}_{tm} &= (\bar{h}_{tp} + \beta\bar{h}_{ts})/(1 + \beta) \\ \sigma_m &= (\sigma_p + \beta\sigma_s)/(1 + \beta) \\ &= (\bar{h}_{tp}/\pi_{tp} + \beta\bar{h}_{ts}/\pi_{ts})/(1 + \beta) \\ \pi_{tm} &= \bar{h}_{tm}/\sigma_m \\ \bar{u}_e &= \left(\frac{2}{1 + \beta}\right)^{1/2} \left[\bar{h}_{tp}\left(1 - \frac{1}{\pi_{tp}}\right) + \beta\bar{h}_{ts}\left(1 - \frac{1}{\pi_{ts}}\right)\right]\end{aligned}\tag{31}$$

In the manner used above for the ejector augmentor, we find the specific thrust and augmentation ratio to be, respectively,

$$f = (1 + \beta)^{\frac{1}{2}} \left(\frac{1}{\mu^2 v^2} + \beta \right)^{\frac{1}{2}} - (1 + \beta) \quad (32)$$

$$\phi = \frac{1}{1 - \mu v} \left[(1 + \beta)^{\frac{1}{2}} (1 + \beta \mu^2 v^2)^{\frac{1}{2}} - (1 + \beta) \mu v \right] \quad (33)$$

where we have introduced the parameters μ and v defined in Equations (13) and (14).

It can be shown, although we will not do it here, that the best performance which can be achieved by a nonmixed-flow turbofan is the same as that given above for the mixed-flow turbofan, and is achieved when the primary and secondary flows have the same exhaust velocities.

5. THE ISENTROPIC COMPRESSOR

Up to this point, we have not made any stipulations concerning the nature of the "pump" which is used to compress captured ambient air from its stagnation conditions to the primary flow reservoir conditions for either the ejector augmentor or the turbofan. The most efficient device for the primary flow pump is an isentropic compressor. (We assume that a suitable power source is available to drive it.) For such a compressor, the parameters μ and v are related, since

$$\pi_{tp} = \pi_{ts} \frac{h_{tp}}{h_{ts}}$$

for isentropic compression. One then finds the relationship

$$v_{isen} = \left[\frac{\pi_{ts} - 1}{\pi_{ts} - \mu^2} \right]^{\frac{1}{2}}$$

from Equations (13) and (14). This may be expressed, using Equation (16), as

$$v_{isen} = \left[\frac{\frac{\gamma-1}{2} M_{\infty}^2}{(1 - \mu^2 + \frac{\gamma-1}{2} M_{\infty}^2)} \right]^{\frac{1}{2}} \quad (34)$$

which shows explicitly the Mach number dependence of the relationship.

6. CORE TURBINE ENGINE GAS GENERATOR

We now assume the "pump" to be a simple turbine engine gas generator, since this is what is most commonly used in practice. With this assumption, we can derive the primary reservoir conditions (\bar{h}_{tp} , π_{tp} , σ_p) in terms of the turbine engine compressor pressure ratio (p_{tc}/p_{ts}) and the combustor temperature rise (ΔT_c).

The T-S diagram for an ideal turbine engine gas generator is shown in Figure 4. We define nondimensional compressor pressure ratio and combustor temperature rise parameters

$$\alpha = (p_{tc}/p_{ts})^{\frac{\gamma-1}{\gamma}}$$

$$\Delta \bar{h}_c = \Delta T_c / T_\infty$$

Then by definition

$$\pi_{tc} = \alpha \pi_{ts}$$

$$\bar{h}_{tt} = \bar{h}_{tc} + \Delta \bar{h}_c$$

and, since the turbine and compressor works must match,

$$(\bar{h}_{tc} - \bar{h}_{ts}) = (\bar{h}_{tt} - \bar{h}_{tp})$$

The compression is assumed to be isentropic, so

$$\bar{h}_{tc} = \bar{h}_{ts} \pi_{ts} / \pi_{tc} = \alpha \bar{h}_{ts}$$

Assuming isentropic expansion in the turbine and solving the above equations, we find

$$\begin{aligned}
c_p &= 1 + \frac{1}{\alpha} \frac{\Delta h_c}{h_{ts}} \\
h_{tp} &= h_{ts} \left(1 + \frac{\Delta h_c}{h_{ts}} \right) \\
\pi_{tp} &= \pi_{ts} \left(1 + \frac{\Delta h_c}{h_{ts}} \right) / \left(1 + \frac{1}{\alpha} \frac{\Delta h_c}{h_{ts}} \right)
\end{aligned} \tag{35}$$

for the primary reservoir conditions. The "temperature" and "pressure" parameters, μ and ν , can be expressed in terms of the turbine engine parameters, α and Δh_c :

$$\begin{aligned}
\mu &= \left[1 + \frac{\Delta h_c}{h_{ts}} \right]^{-\frac{1}{\alpha}} \\
\nu &= \left[1 + (1 - \mu^2) \left(1 - \frac{1}{\alpha} \right) / (\pi_{ts} - 1) \right]^{-\frac{1}{2}}
\end{aligned} \tag{36}$$

Since

$$h_{ts} = \pi_{ts} = 1 + \frac{\gamma-1}{2} M_\infty^2$$

the relationship between (μ, ν) and $(\alpha, \Delta h_c)$, and hence between (f, ϕ) and $(\alpha, \Delta h_c)$, are Mach number dependent.

Finally, if the compressor pressure ratio is made infinitely large then the turbine engine gas generator becomes, in essence, an isentropic compressor. This can be seen by examining Equations (35) and (36) in the limit $(\alpha \rightarrow \infty)$.

SECTION III

DISCUSSION

1. MAXIMUM THRUST AUGMENTATION AND THE TURBOFAN

In his analysis, Heiser obtained results for the maximum performance of a passive augmentor which are essentially the same as those we have derived in Section II.4 for the ideal turbofan. However, it is theoretically possible to exceed the maximum performance found by Heiser by using energy transfer processes which are thermodynamically reversible.⁽⁴⁾ Examples of thermodynamically reversible devices are ideal turbocompressors and ideal counterflow heat exchangers (under some conditions). In the Appendix, it is shown that the maximum augmentation ratio achievable by a passive augmentor using reversible thermodynamic processes is

$$\phi_{\max} = \frac{[1 + \beta]^{\frac{1}{2}} [(\bar{h}_{tp} + \beta \bar{h}_{ts}) - (1 + \beta) \sigma_p \frac{1}{1+\beta}]^{\frac{1}{2}} - [1 + \beta] [\bar{h}_s - 1]^{\frac{1}{2}}}{[\bar{h}_{tp} - \sigma_p]^{\frac{1}{2}} - [\bar{h}_{ts} - 1]^{\frac{1}{2}}}$$

for given initial flow conditions ($\beta, \bar{h}_{tp}, \bar{h}_{ts}, \sigma_p, \sigma_s = 1$). This equation unfortunately, unlike those for the ejector augmentor and turbofan, cannot be cast into a Mach number-independent form in terms of the temperature and pressure parameters μ and ν . Because of this, because the ideal mixed-flow turbofan performance is only slightly worse (~5%) than the theoretical maximum for practical flow conditions and because the turbofan is the most common form of passive thrust augmentor, we will use the ideal mixed-flow turbofan as the standard for comparison in the following discussion.

2. COMPARISON OF ENTROPIES

The first comparison we make is between the nondimensional entropies of the mixed flows for the ejector augmentor and the turbofan. From Equations (11) and (31):

$$\Delta \sigma_m = \sigma_{mej} - \sigma_{mtf} = \frac{\beta}{(1+\beta)^2} (\bar{h}_{tp} - \bar{h}_{ts}) \left(\frac{1}{\pi_{ts}} - \frac{1}{\pi_{tp}} \right)$$

This is always positive if $T_{tp} \geq T_{ts}$ and $P_{tp} \geq P_{ts}$. (If $T_{tp} < T_{ts}$ and $P_{tp} \geq P_{ts}$, then the second solution given in Equation (10) for the optimum mixing pressure must be used, which gives the result $\Delta\sigma_m = 0$.) Therefore, an ideal ejector augmentor with complete mixing can never be more efficient than an ideal turbofan for the same $(\beta, T_{tp}, P_{tp}, T_{ts}, P_{ts})$. This is not unexpected since the mixing in the ideal turbofan occurs at negligible velocity, while the mixing in the ejector generally occurs at high relative velocities.

3. IDEAL PERFORMANCE CONTOUR MAPS

In Figure 5*, we present constant specific thrust and constant augmentation ratio contours for ideal ejector augmentors, plotted as functions of μ and ν for various mass flow ratios using Equations (17) and (18). The most obvious feature of the figure is that, when $\mu = \nu$, the augmentation ratio is unity; that is, no thrust augmentation is realized. The reason for this is as follows:

When $\mu = \nu$, the optimum mixing pressure, given by Equation (10), is equal to the ambient static pressure ($\pi^* = 1$). Now, in an ejector with constant pressure mixing, no net thrust is developed in the mixer (conservation of momentum); the thrust augmenting forces are developed in the inlet, the secondary flow nozzle and the exhaust nozzle. If the mixing occurs at ambient static pressure, then, from conservation of momentum, the secondary flow cannot develop any net thrust in either the inlet and secondary flow nozzle, or the exhaust nozzle; hence, there can be no thrust augmentation of the primary flow.

A second feature of the contour maps in Figure 5 and of Equations (17) and (18), is the symmetry in μ and ν of both the specific thrust and augmentation ratio contours (diagonal symmetry).

*The reader should bear in mind that this figure and those to follow, do not show the performance of a single augmentor. Rather, each point in the figures represents the performance of a different optimized ideal augmentor.

As can be seen in the figure, for ideal ejector augmentors the maximum value of the augmentation ratio for a particular mass flow ratio β is obtained when (μ, ν) is $(0, 1)$ or $(1, 0)$. From Equation (18), this value is

$$\phi_{\max} = (1 + \beta)^{\frac{1}{2}}$$

Thus, the augmentation ratio theoretically attainable by an ideal ejector augmentor, which uses compressible gasses and a constant pressure mixer, can exceed the limiting value of two which Heiser found assuming incompressible flow and constant area mixing.

For an ideal ejector, the case $\mu = 1$ (i.e., $T_{tp} = T_{ts}$) is that of a "pure ejector," that is, an ejector in which the energy added to the bypass flow comes entirely from the pressure of the primary flow. The case $\nu = 1$ (i.e., $p_{tp} = p_{ts}$) is that of a "pure ramjet"; the only energy added to the bypass flow is thermal energy from the primary flow. For this reason, we refer to the region of the μ - ν map which lies above the diagonal ($\mu > \nu$) in Figure 5 as the "ejector side" of the map and the region below the diagonal ($\mu < \nu$) as the "ramjet side." The optimum mixing pressure, as given by Equation (10), is below the ambient static pressure on the ejector side and above ambient on the ramjet side. In the limits, the optimum mixing pressure for the pure ejector is zero, and for the pure ramjet, the freestream total pressure.

Since the energy (fuel) consumption is more or less proportional to the stagnation temperature difference between the primary and secondary flows, one would prefer an ejector device which operates on the ejector, rather than ramjet, side of the map, where the total temperature difference is low (μ near unity).

In Figure 6, we show constant specific thrust and augmentation ratio contours for several mass flow ratios for the ideal mixed-flow turbofan, as given by Equations (32) and (33).

Comparison of this figure with Figure 5 shows a striking difference in the augmentation ratio contours. In particular, for the turbofan, useful augmentation can be obtained anywhere in the region of the maps, whereas, for the ejector augmentor, useful augmentation can be obtained only away from the diagonal ($\mu=v$).

4. MACH NUMBER DEPENDENCE OF LIMITS ON PERFORMANCE

Although the specific thrust and augmentation ratio contours of Figures 5 and 6 are not Mach number dependent, the values of μ and v are (for specified p_{tp} and T_{tp}). In particular, the theoretically accessible region of the figures is Mach number dependent, since v has a limiting non-zero value as the primary total pressure becomes infinitely large. From Equations (14) and (16),

$$v_{\min}(M_{\infty}) = \frac{\frac{\gamma-1}{2}M_{\infty}^2}{(1 + \frac{\gamma-1}{2}M_{\infty}^2)^{1/2}}$$

This is a mathematical limit and contains no assumptions concerning the thrust augmentation device (other than that v is a valid parameter for describing its performance). Thus, it is equally applicable to the ideal turbofan and to the ideal ejector augmentor. The consequence of this minimum attainable v is that the regions of high augmentation ratio along the left border of the μ - v maps are beyond reach unless the flight Mach number is low. The regions of high augmentation ratio along the lower boundary are practically unattainable because the required primary flow total temperature is too high:

$$T_{tp} = T_{\infty} (1 + \frac{\gamma-1}{2}M_{\infty}^2) \frac{1}{\mu^2}$$

(from Equations (13) and (16)). If, for the sake of illustration, we choose a maximum practical value of nine for T_{tp}/T_{∞} , then

$$\mu_{\min} = \frac{1}{3} (1 + \frac{\gamma-1}{2}M_{\infty}^2)^{1/2}$$

This and v_{\min} , which is defined above, define accessible regions of the μ - v maps as functions of the freestream Mach number. These regions are shown in Figure 7 for selected Mach numbers. This figure may be overlaid on the μ - v maps of Figures 5 and 6 to see, graphically, the effect of the Mach number on the attainable performance for ideal ejector augmentors and turbofans.

5. EJECTOR AUGMENTOR WITH AN ISENTROPIC COMPRESSOR

We now examine the case in which the primary "pump" of our ideal thrust augmentors is an isentropic compressor. In Figure 8, are shown the μ - v curves for isentropic compressors for various Mach numbers, as given by Equation (34). The horizontal tick mark on each curve is at the value of μ for which $T_{tp}/T_{\infty} = 9$, the temperature used previously in Figure 7. As with Figure 7, this figure may be overlaid on any of the maps of Figures 5 and 6. As one would expect, the use of an isentropic compressor further restricts the accessible regions of the μ - v maps. This restriction is particularly bad for low primary stagnation temperatures ($\mu \approx 1$) where the ejector augmentor performance is best. The effect on turbofan performance is not as severe because the turbofan has good performance near the μ - v diagonal, whereas the ejector augmentor does not.

Since an ideal turbine engine gas generator with infinite compressor pressure ratio is an isentropic compressor, and since an ideal turbofan is at best an isentropic compressor, Figure 8 also represents the outer limits for the accessible regions of the μ - v maps for turbine engines and turbofans used as primary "pumps." (We project this statement, without proof, to include all heat engines.) As a result, Figure 8 overlaid on any of the maps of Figures 5 and 6 will show the theoretical limits of ejector augmentor and turbofan performance for the given Mach numbers and mass flow ratio.

6. EJECTOR AUGMENTOR WITH TURBINE ENGINE GAS GENERATOR

Finally, we consider the case in which the primary "pump" is a simple turbine engine gas generator, as described in Section II.6. In Figure 9, constant specific thrust and augmentation ratio contours are shown for a mass flow ratio of five at Mach numbers of 0.2, 0.7 and 1.4, plotted as functions of the gas turbine compressor pressure ratio and the combustor temperature rise. The contours were obtained from Equations (17), (18) and (36). In these maps, the area to the right of the $\phi = 1$ contour is on the ejector side and the area to the left is on the ramjet side, as defined above. As can be seen, for the low Mach number case, useful thrust augmentation can be obtained. However, the maximum augmentation requires an unrealistically low combustor temperature rise in the turbine engine. (Such a low temperature rise would make the gas generator too large and heavy.) As the temperature is raised to more reasonable levels, the thrust augmentation is reduced, but remains useful. For higher Mach numbers, the attainable augmentation drops to practically useless levels. At supersonic Mach numbers, some thrust augmentation is realized on the ramjet side, but this is a relatively useless benefit, because higher thrust can be achieved for the same fuel consumption (which is proportional to combustor temperature rise) simply by raising the compressor pressure ratio and forgetting about the augmentor device.

To further clarify the relationship between the Mach number-independent maps of Figure 5 and the Mach number-dependent maps of Figure 9, we have plotted in Figure 10 the boundaries of the temperature rise - pressure ratio region of the maps of Figure 9 as functions of μ and v for selected Mach numbers. This figure is similar in concept to Figures 7 and 8. For each Mach number, the region of interest is to the right of the curved line, which is itself the contour for compressor pressure ratio equal to 32. These curves are independent of mass flow ratio and may be overlaid on both the ejector augmentor and turbofan maps of Figures 5 and 6. Comparing Figures 8 and 10, we see that the use of a gas turbine as a core device further restricts the accessible regions of the μ - v performance maps for both ejector augmentors and turbofans.

SECTION IV

CONCLUSIONS

The preceding analyses and discussion have all focused on the maximum performance which is theoretically attainable by ejector thrust augmentors. All flow processes were assumed to be isentropic, except for the flow mixing, which cannot be isentropic due to the second law of thermodynamics. The performance of real ejector augmentors will not be as good because of viscous and heat transfer losses, shock losses, incomplete mixing, non-optimum mixing conditions, etc. For this reason and considering the results of the present analytic study, we cannot be very optimistic about the efficacy of ejector devices for thrust augmentation for other than relatively low subsonic flight Mach numbers. We have found that the turbofan offers better performance than does the ejector augmentor for all forward flight conditions (for the same mass flow ratios).

As a result of this study, we have drawn the following conclusions:

- The ejector augmentor is theoretically capable of respectable performance. However, this performance is severely degraded if the primary flow is hot.
- The turbine engine is not a particularly suitable "pump" for an ejector augmentor because the turbine engine exhaust gases are too hot, and as a result, degrade the potential ejector performance to nearly useless levels, except at low Mach numbers. We may also turn this statement around: Ejector devices are not very suitable for thrust augmentation of turbine engines, except at low subsonic Mach numbers. (This conclusion also applies to isentropic compressors and turbofans used as pumps for ejector devices.)
- As the flight Mach number increases, the performance of an ejector augmentor is degraded faster than that of a turbofan.

The ejector augmentor should be most beneficial for lift and thrust enhancement at low speeds (e.g., V/STOL operations). It may also be useful for some special applications where geometric considerations mitigate against the use of a turbofan. However, the turbofan will probably remain the better device in terms of performance, because of its advanced state of development and high component efficiencies.

Lest these conclusions be assumed to apply to all ejector-like devices, we close with the following caveat:

We have assumed throughout this study of ejector thrust augmentors that the primary and secondary flows are completely mixed and that all momentum and energy transfer processes occur in the mixer. For ejector-like devices for which these assumptions do not apply (e.g., the so-called "jet compressor"), our conclusions do not necessarily apply either.

APPENDIX

MAXIMUM THRUST AUGMENTATION

Assume that we have two fluid flows - a primary flow with initial stagnation conditions (h_{tp}, s_p) and a secondary flow with initial stagnation conditions (h_{ts}, s_s) - with a secondary/primary mass flow ratio β . Further assume that the two flows interact and proceed through some thermodynamic processes to final stagnation conditions (h'_{tp}, s'_p) and (h'_{ts}, s'_s) . The two flows are then expanded isentropically through nozzles to ambient static pressure to provide thrust.

The exhaust velocities of the two flows are given by

$$\begin{aligned} u_{ep} &= \sqrt{2} [h'_{tp} - h'_{ap}]^{\frac{1}{2}} \\ u_{es} &= \sqrt{2} [h'_{ts} - h'_{as}]^{\frac{1}{2}} \end{aligned} \tag{A.1}$$

where h'_{ap} and h'_{as} are static enthalpies at ambient static pressure:

$$\begin{aligned} h'_{ap} &= h_{\infty} e^{(s'_p - s_{\infty})/C_p} \\ h'_{as} &= h_{\infty} e^{(s'_s - s_{\infty})C_p} \end{aligned} \tag{A.2}$$

The resultant specific thrust is

$$f = (u_{ep} + \beta u_{es})/u_{\infty} - (1 + \beta) \tag{A.3}$$

The initial and final stagnation conditions are related by the laws of thermodynamics,

$$\begin{aligned} h'_{tp} + \beta h'_{ts} &= h_{tp} + \beta h_{ts} \\ s'_p + \beta s'_s &\geq s_p + \beta s_s \end{aligned} \tag{A.4}$$

The latter inequality can be written as

$$s'_p + \beta s'_s = s_p + \beta s_s + (1 + \beta) C_p \epsilon \quad (\text{A.5})$$

where $\epsilon \geq 0$.

We now seek the maximum specific thrust for fixed initial flow conditions by varying first h'_{tp} , then s'_p and finally ϵ . Using Equations (A.1) through (A.4), the first variation

$$\frac{\partial f}{\partial h'_{tp}} = 0$$

has the solution

$$h'_{tp} = h_{tp} - \frac{\beta}{1+\beta} [h_{tp} - h'_{ap} - h_{ts} + h'_{as}]$$

which gives upon substitution into Equations (A.1) and (A.3):

$$u_{ep} = u_{es} = \left(\frac{2}{1+\beta}\right)^{\frac{1}{2}} [h_{tp} + \beta h_{ts} - (h'_{ap} + \beta h'_{as})]^{\frac{1}{2}}$$

Using this result and Equation (A.5) in Equation (A.3), the second variation

$$\frac{\partial f}{\partial s'_p} = 0$$

is performed, which gives

$$s'_p = s'_s = \frac{s_p + \beta s_s}{1+\beta} + C_p \epsilon$$

and thence,

$$h'_{tp} = h'_{ts} = \frac{h_{tp} + \beta h_{ts}}{1+\beta}$$

The specific thrust is

$$f = \sqrt{2(1+\beta)} [h_{tp} + \beta h_{ts} - (1+\beta)h_{\infty} e^{(\frac{s_p + \beta s_s}{1+\beta} - s_{\infty})/C_p} e^{\epsilon}]^{1/2} / u_{\infty} - (1+\beta)$$

Cursory examination of this expression shows that the specific thrust is maximized when $\epsilon = 0$, that is, when the flow processes are reversible.

Finally, assuming isentropic diffusion in the inlet ($s_s = s_{\infty}$), we obtain for the maximum attainable specific thrust:

$$f_{\max} = [\frac{1+\beta}{h_{ts}-1}]^{1/2} [h_{tp} + \beta h_{ts} - (1+\beta)\sigma_p^{1/(1+\beta)}]^{1/2} - (1+\beta)$$

where we have introduced the nondimensional parameters used in Section II. The process which gives this maximum performance is one in which the two initial flows interact through a reversible thermodynamic process to move to the same final thermodynamic state, i.e.,

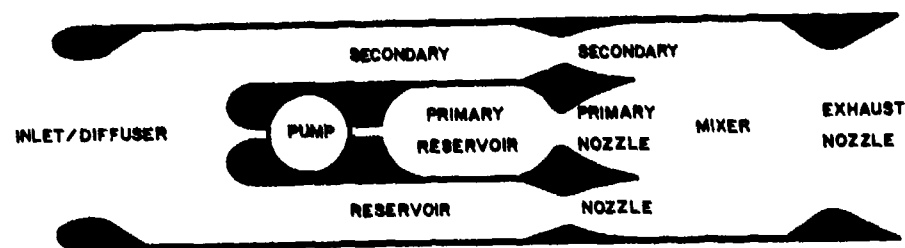
$$h'_{tp} = h'_{ts}$$

$$s'_p = s'_s$$

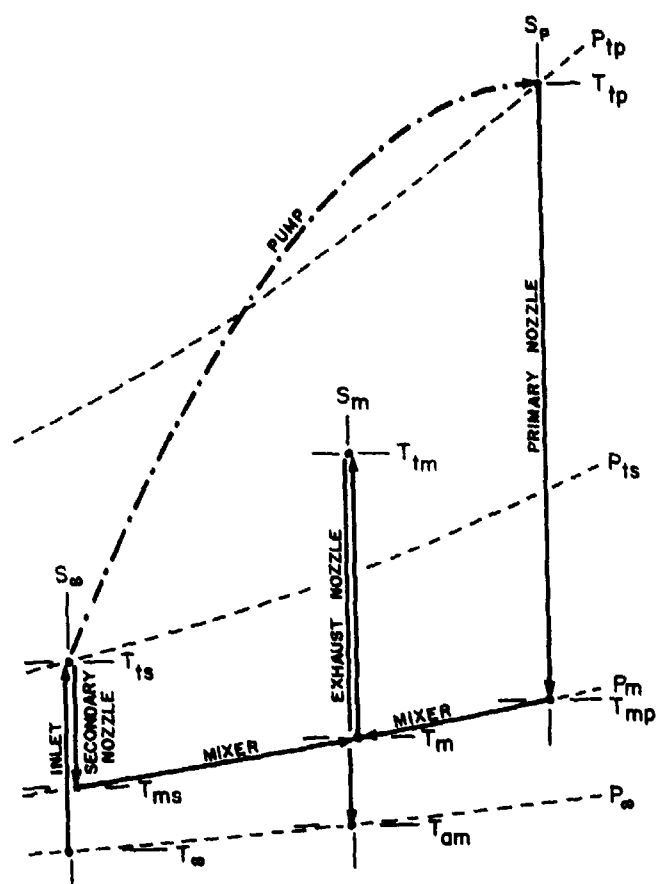
$$\epsilon = 0$$

The augmentation ratio is

$$\phi_{\max} = \frac{[1+\beta]^{1/2} [(h_{tp} + \beta h_s) - (1+\beta)\sigma_p^{1/(1+\beta)}]^{1/2} - [1+\beta][h_{ts} - 1]^{1/2}}{[h_{tp} - \sigma_p]^{1/2} - [h_{ts} - 1]^{1/2}}$$

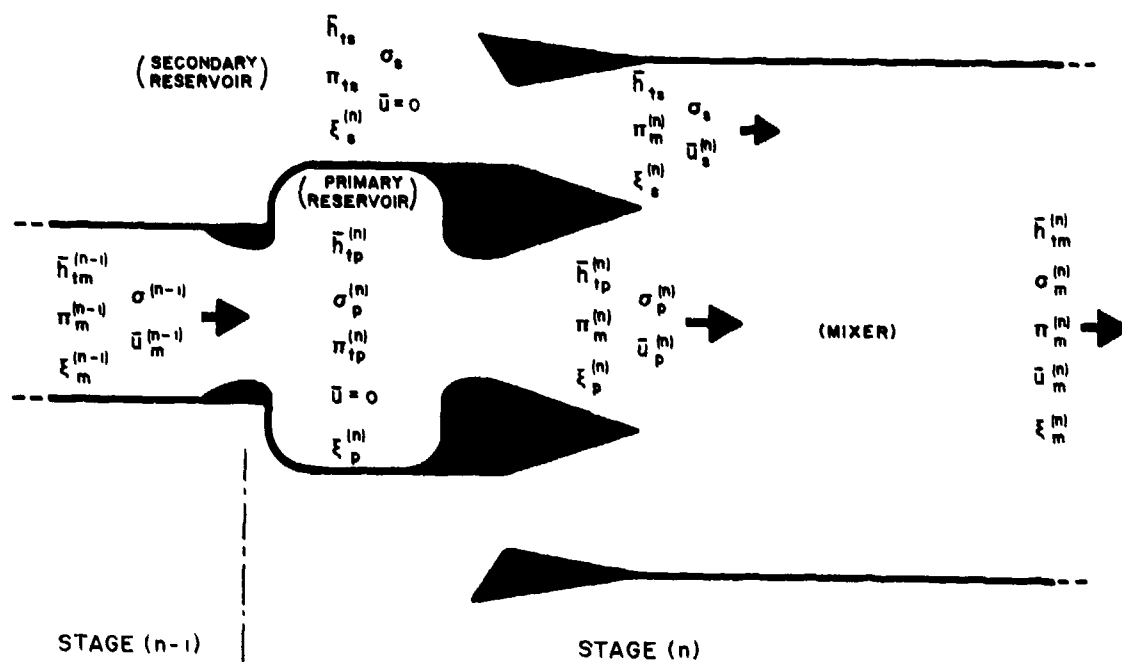


d) SCHEMATIC DRAWING

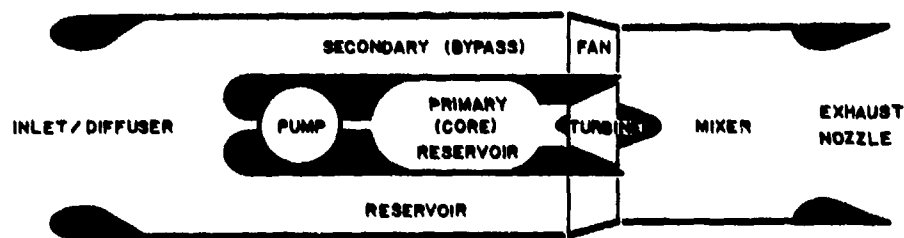


b) T-S DIAGRAM

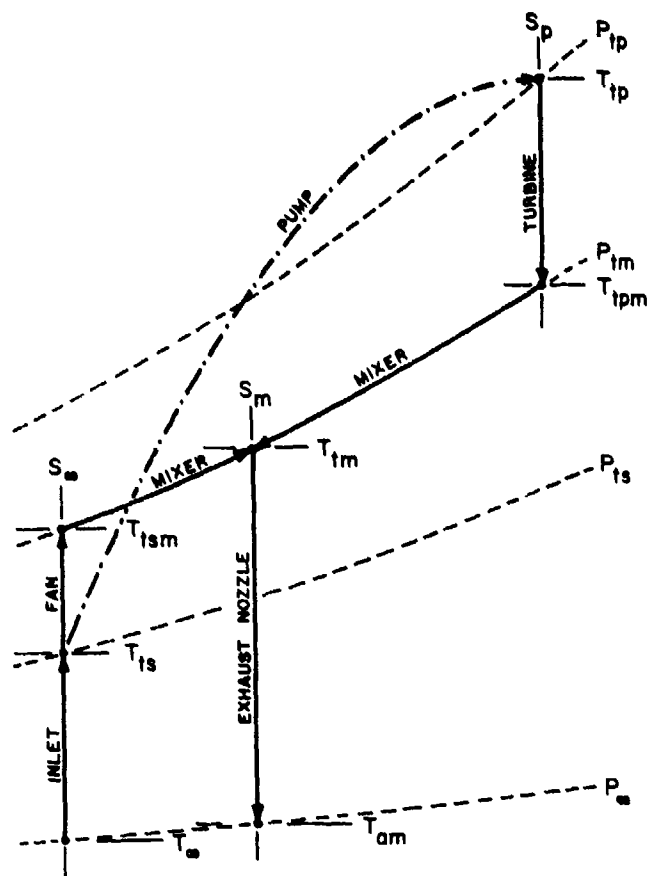
FIGURE 1 Ejector Thrust Augmentor



、 FIGURE 2 Schematic of One Stage of a Multi-Stage Ejector Augmentor



a) SCHEMATIC DRAWING



b) T-S DIAGRAM

FIGURE 3 Turbofan Engine

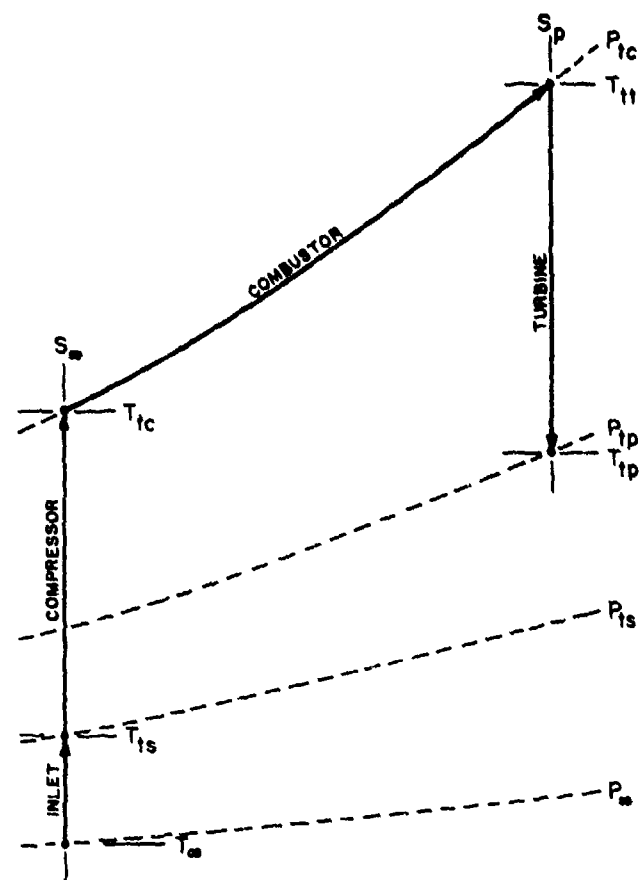


FIGURE 4 T-S Diagram for an Ideal Turbine Engine Gas Generator

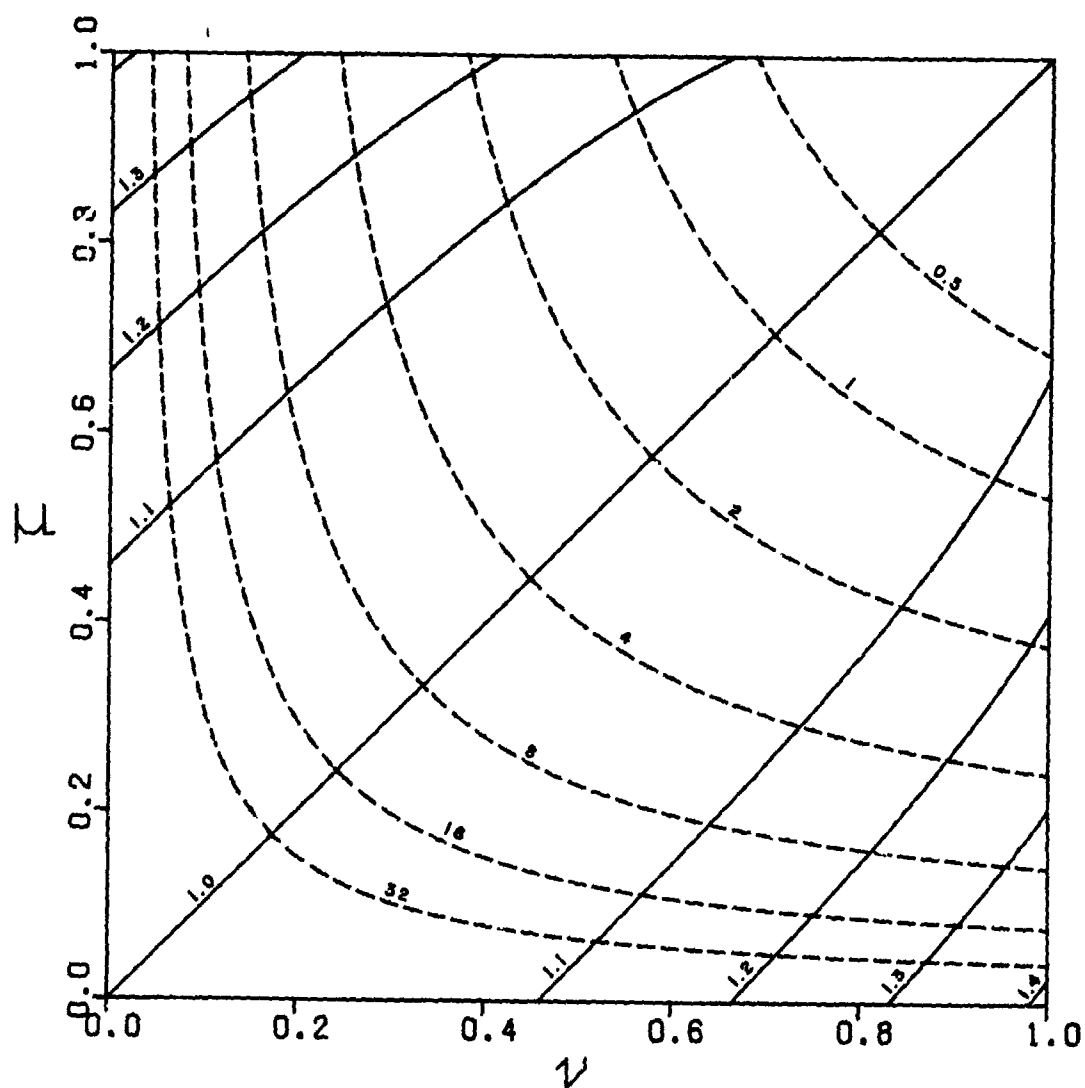


FIGURE 5 Performance Maps for Ideal Ejectors

a) Secondary/Primary Mass Flow Ratio $\beta = 1$
 (—Augmentation Ratio ϕ , ---Specific Thrust f)

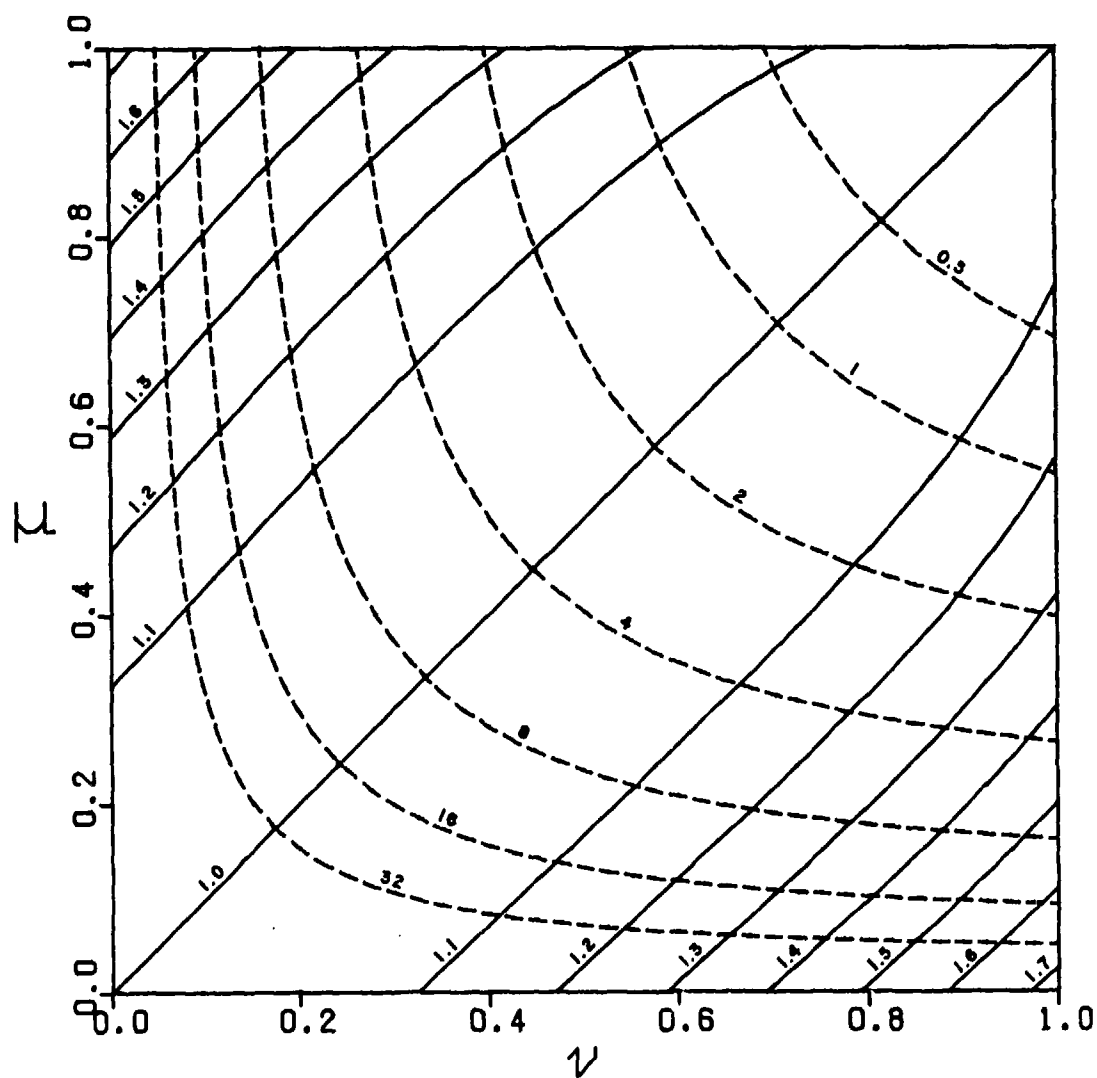


FIGURE 5 Performance Maps for Ideal Ejectors

b) Secondary/Primary Mass Flow Ratio $\beta = 2$
 (—Augmentation Ratio ϕ , ---Specific Thrust f)

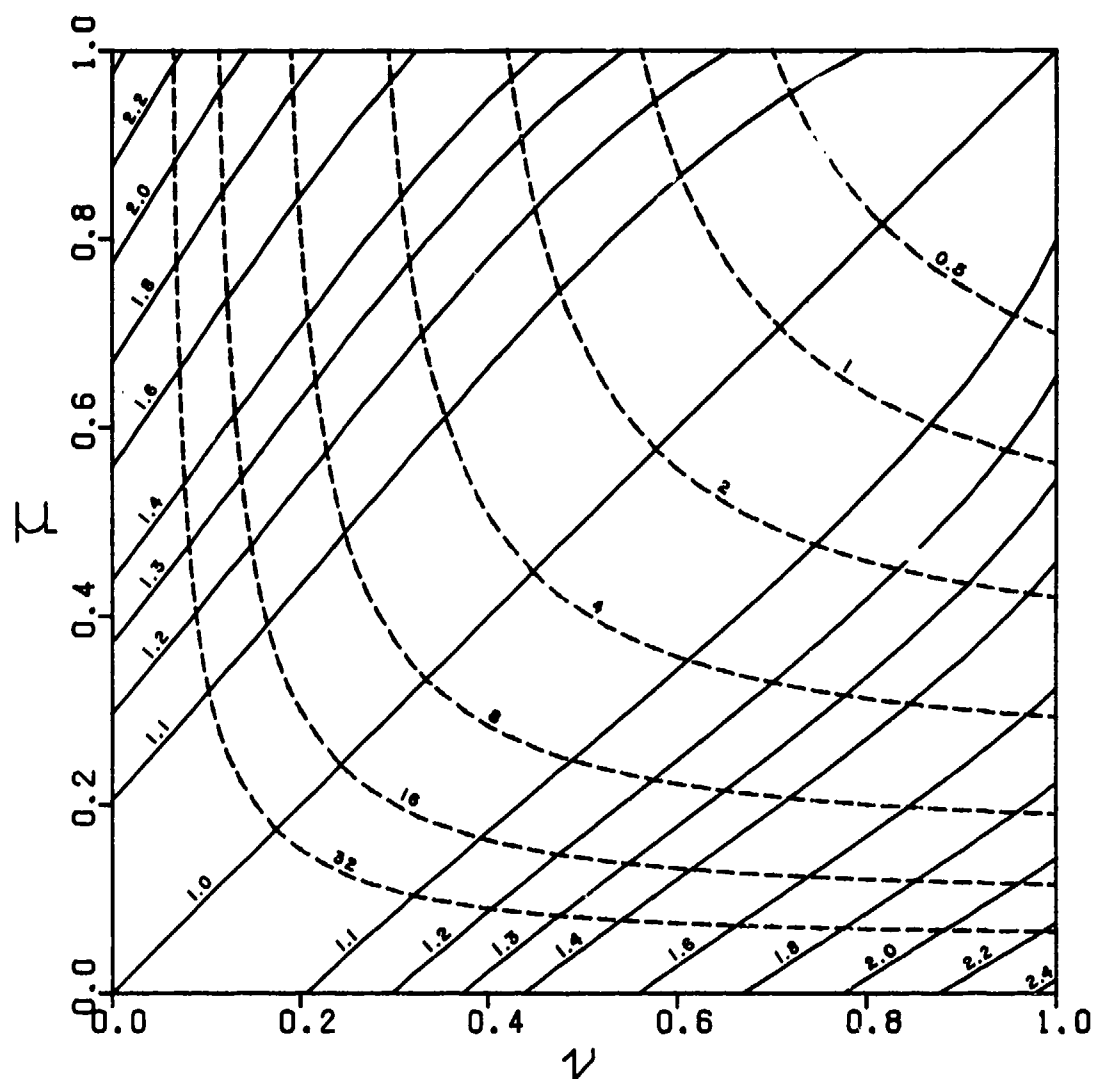


FIGURE 5 Performance Maps for Ideal Ejectors

c) Secondary/Primary Mass Flow Ratio $\beta = 5$
 (—Augmentation Ratio ϕ , ---Specific Thrust f)

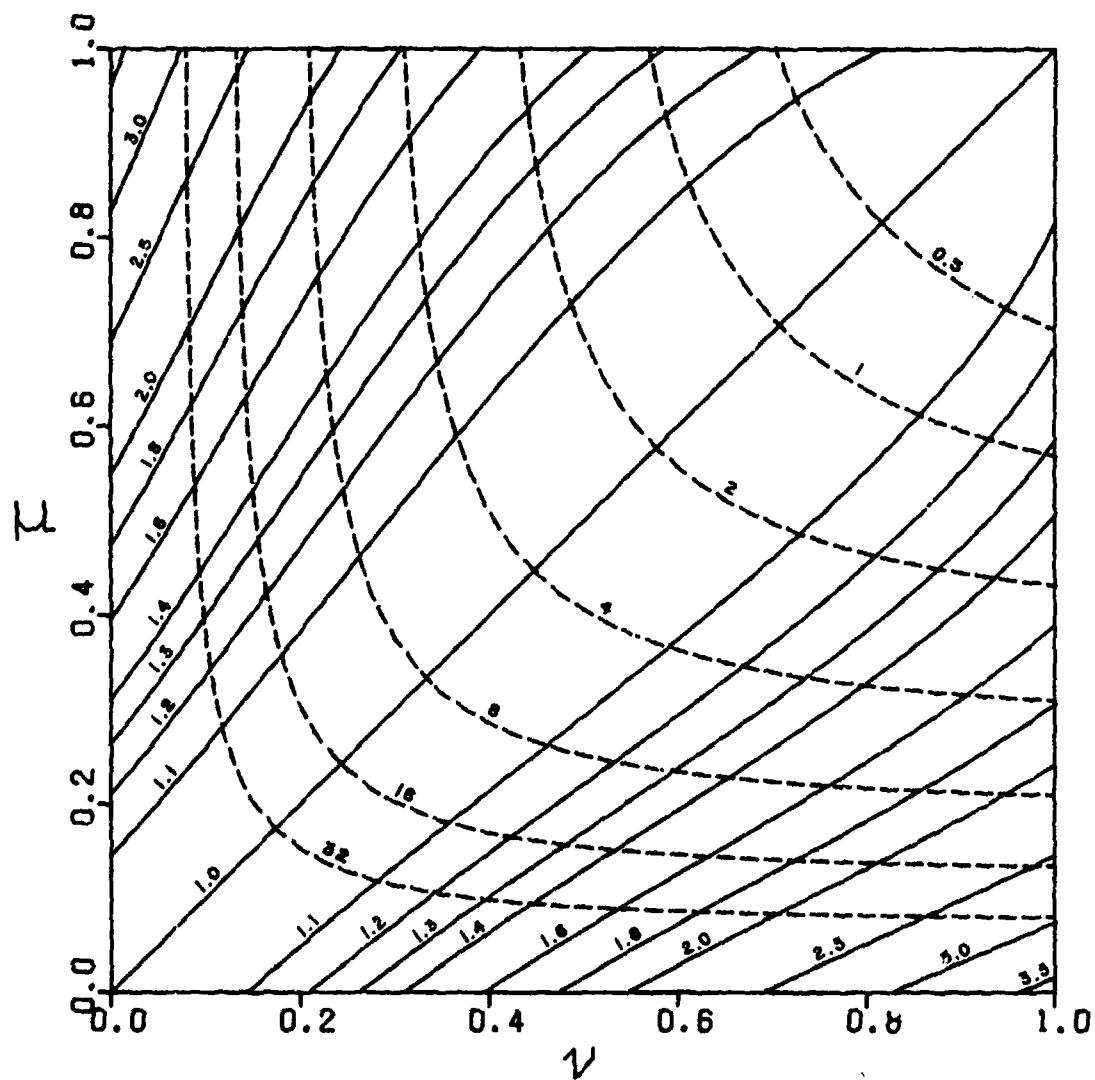


FIGURE 5 Performance Maps for Ideal Ejectors

d) Secondary/Primary Mass Flow Ratio $\beta = 10$
 (—Augmentation Ratio ϕ , ---Specific Thrust f)

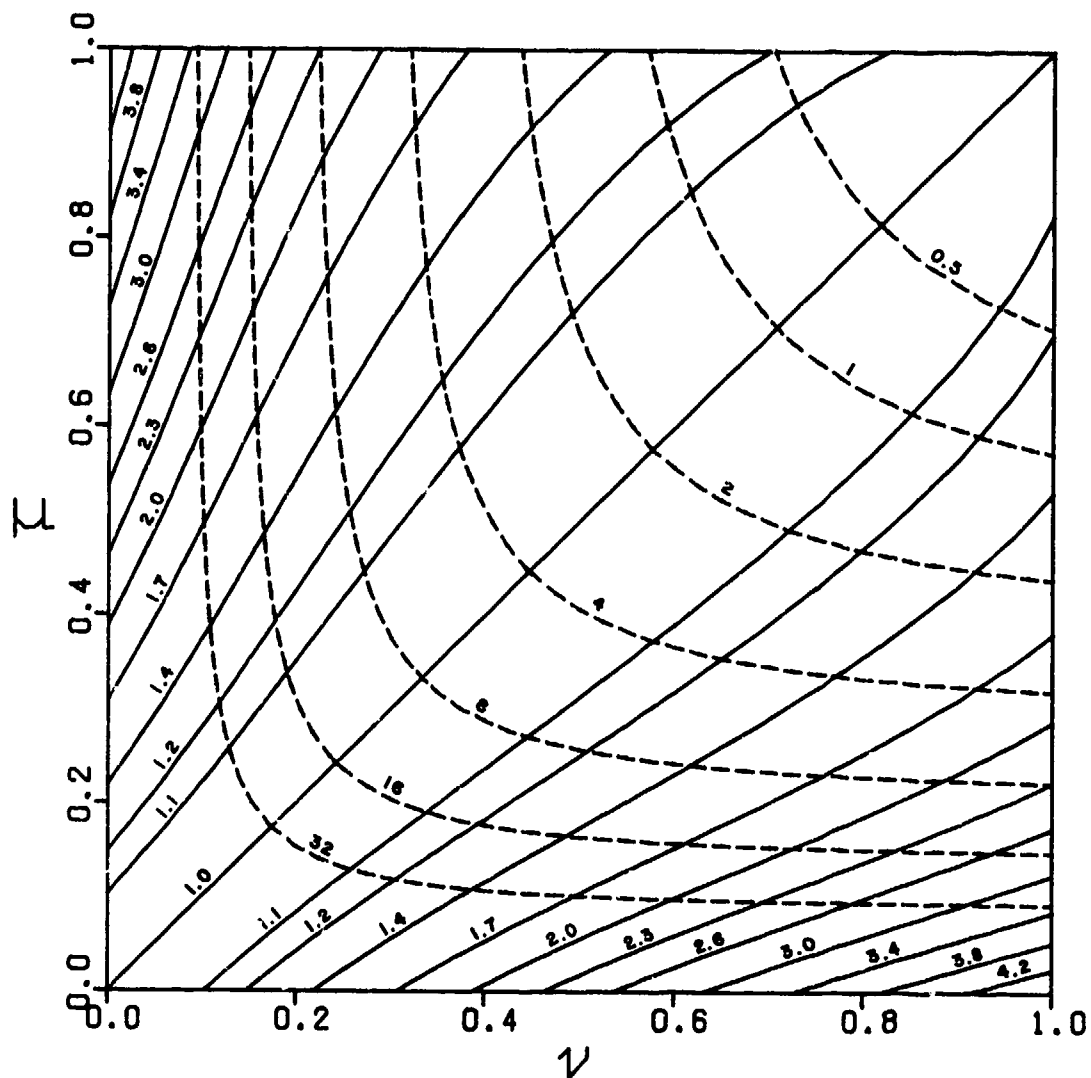


FIGURE 5 Performance Maps for Ideal Ejectors

e) Secondary/Primary Mass Flow Ratio $\beta = 20$
 (—Augmentation Ratio ϕ , ---Specific Thrust f)

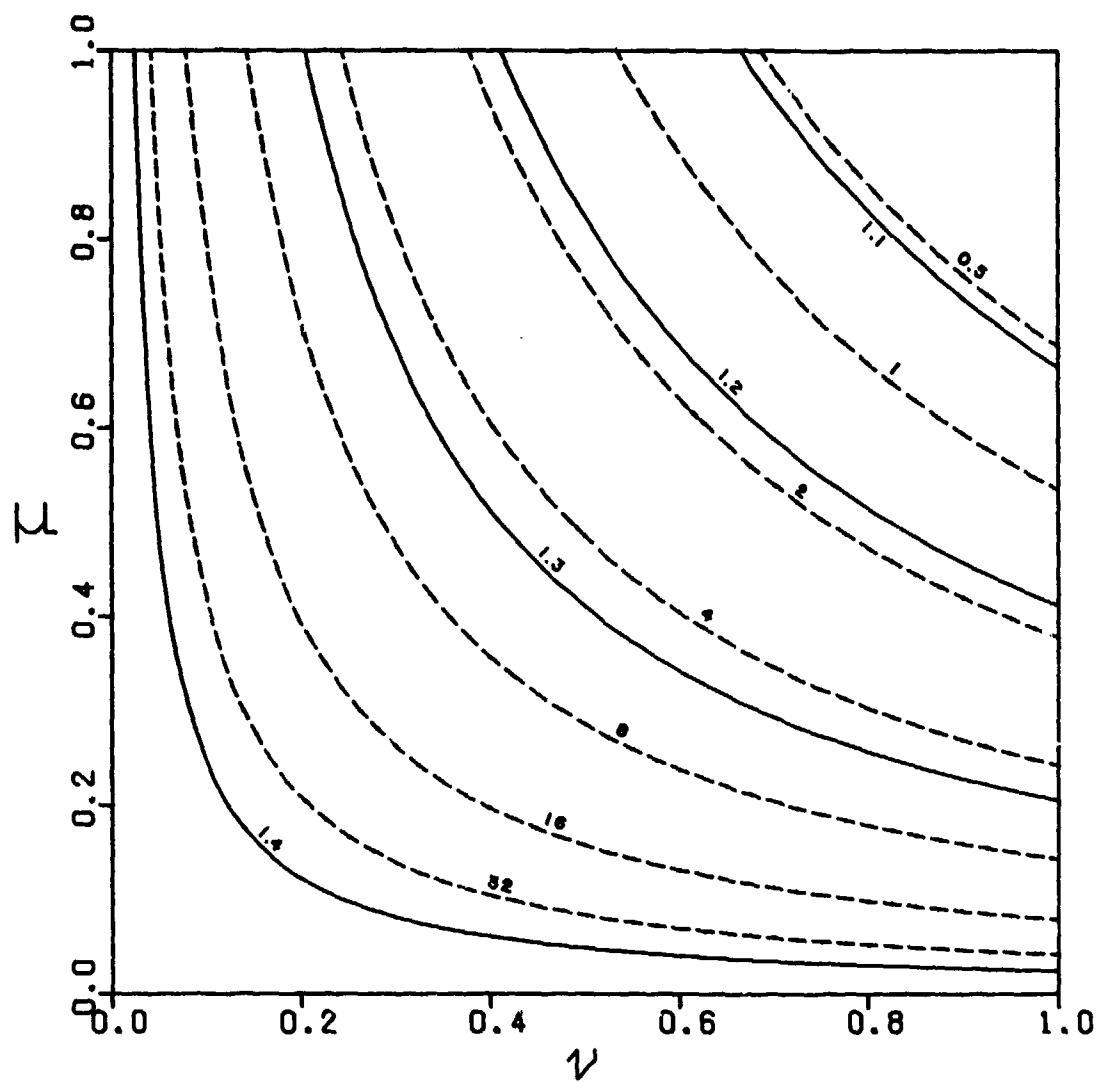


FIGURE 6 Performance Maps for Ideal Turbofans

a) Secondary/Primary Mass Flow Ratio $\beta = 1$
 (—Augmentation Ratio ϕ , ---Specific Thrust f)

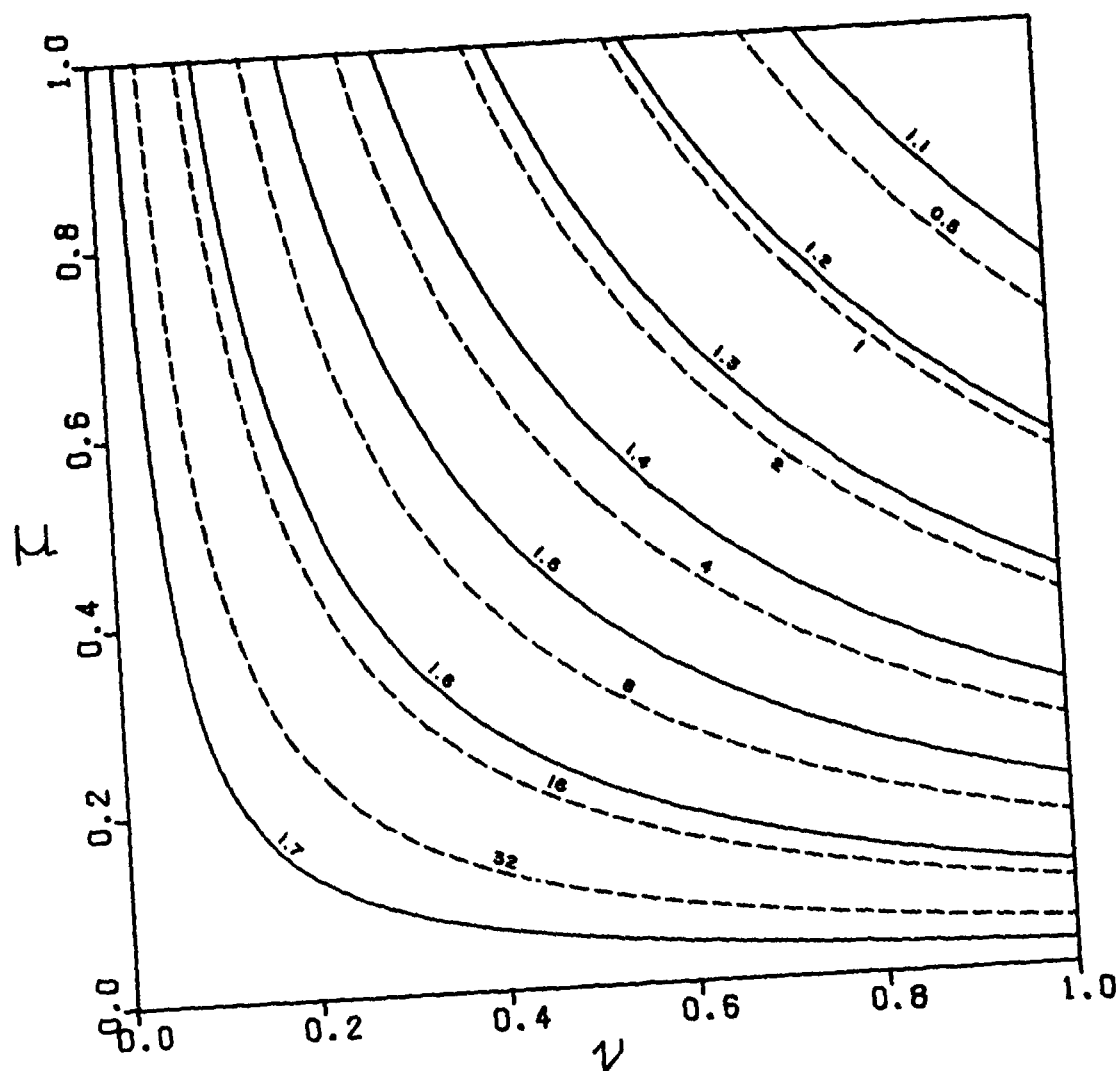


FIGURE 6 Performance Maps for Ideal Turbofans
 b) Secondary/Primary Mass Flow Ratio $\beta = 2$
 (—Augmentation ϕ , ---Specific Thrust f)

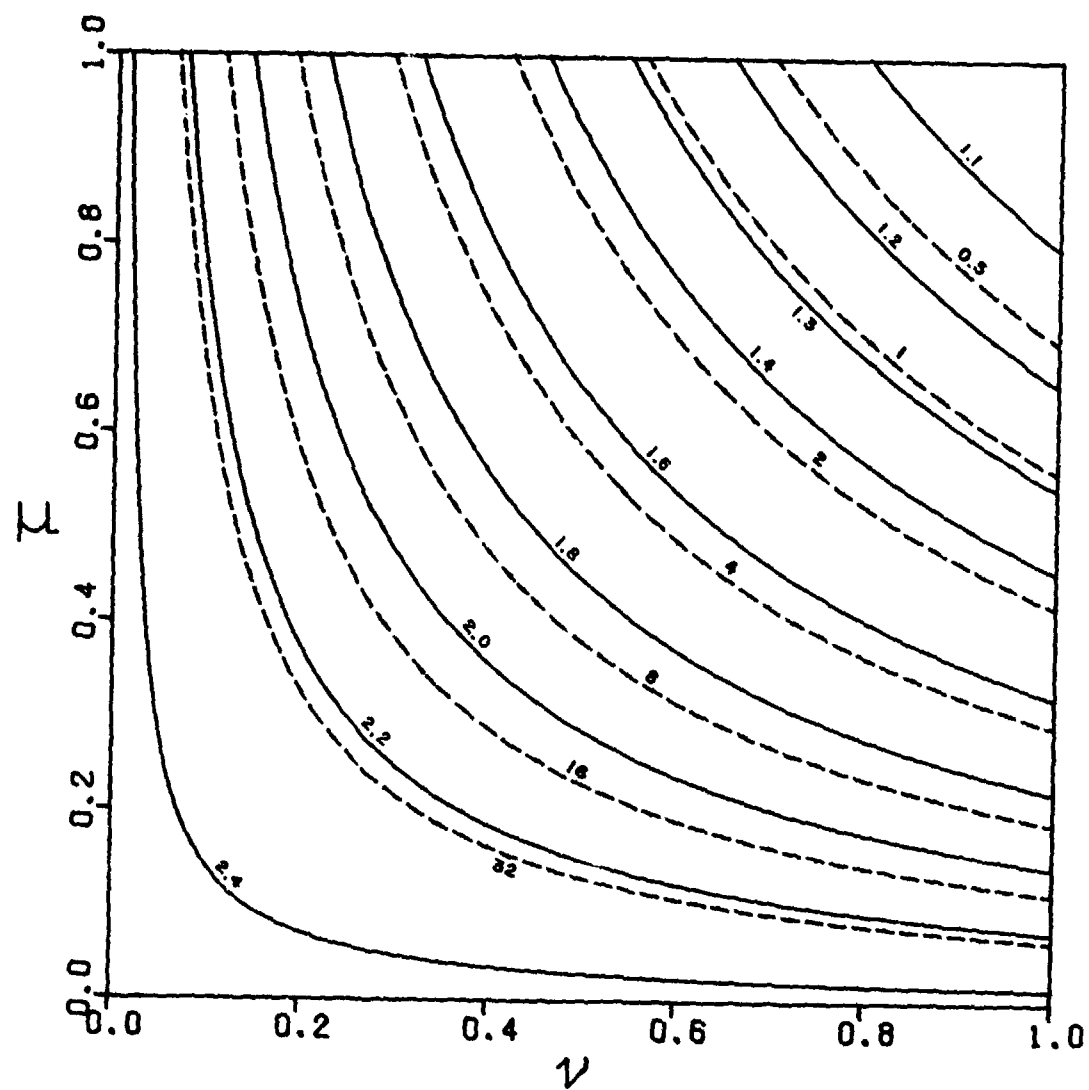


FIGURE 6 Performance Maps for Ideal Turbofans

c) Secondary/Primary Mass Flow Ratio $\beta = 5$
 (—Augmentation ϕ , ---Specific Thrust f)

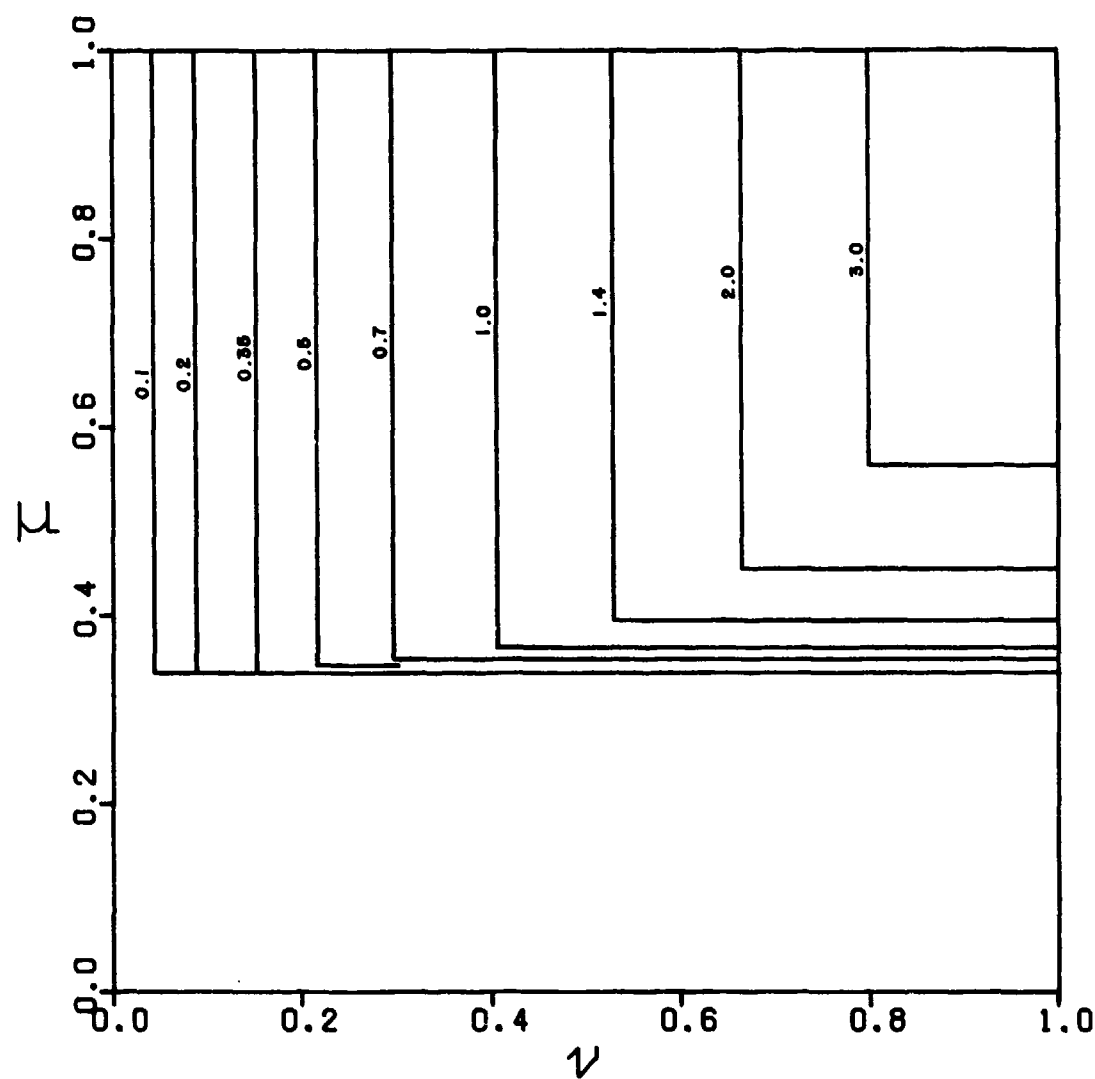


FIGURE 7 Attainable Regions of Performance Maps for Various Mach Numbers

(The regions are to the right of the curves.)

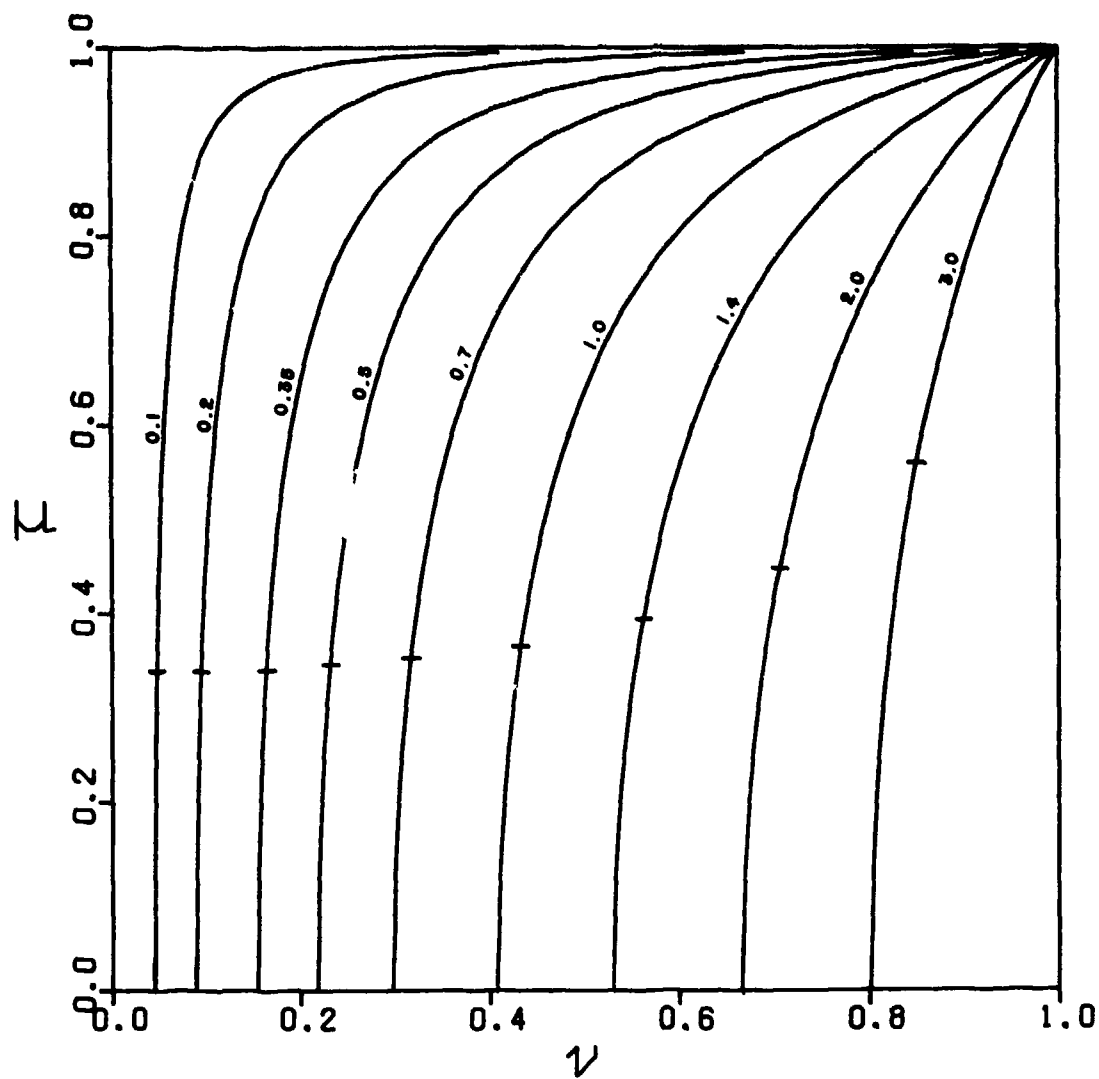


FIGURE 8 Isentropic Compressor Curves for Various Mach Numbers

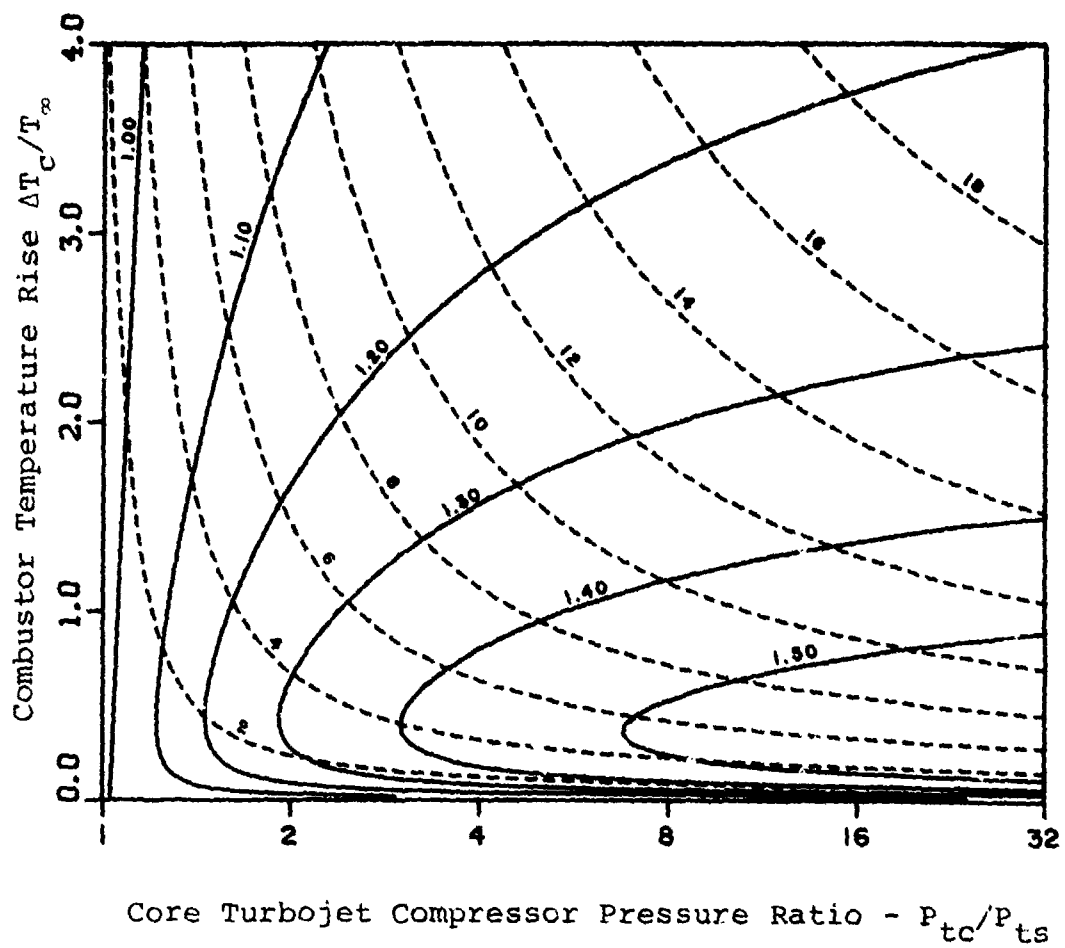


FIGURE 9 Performance Map for Ideal Ejectors with Turbine Engine Cores (Secondary/Primary Mass Flow Ratio $\beta = 5$)

a) Mach Number $M_\infty = 0.2$
 (—Augmentation Ratio ϕ , ---Specific Thrust f)

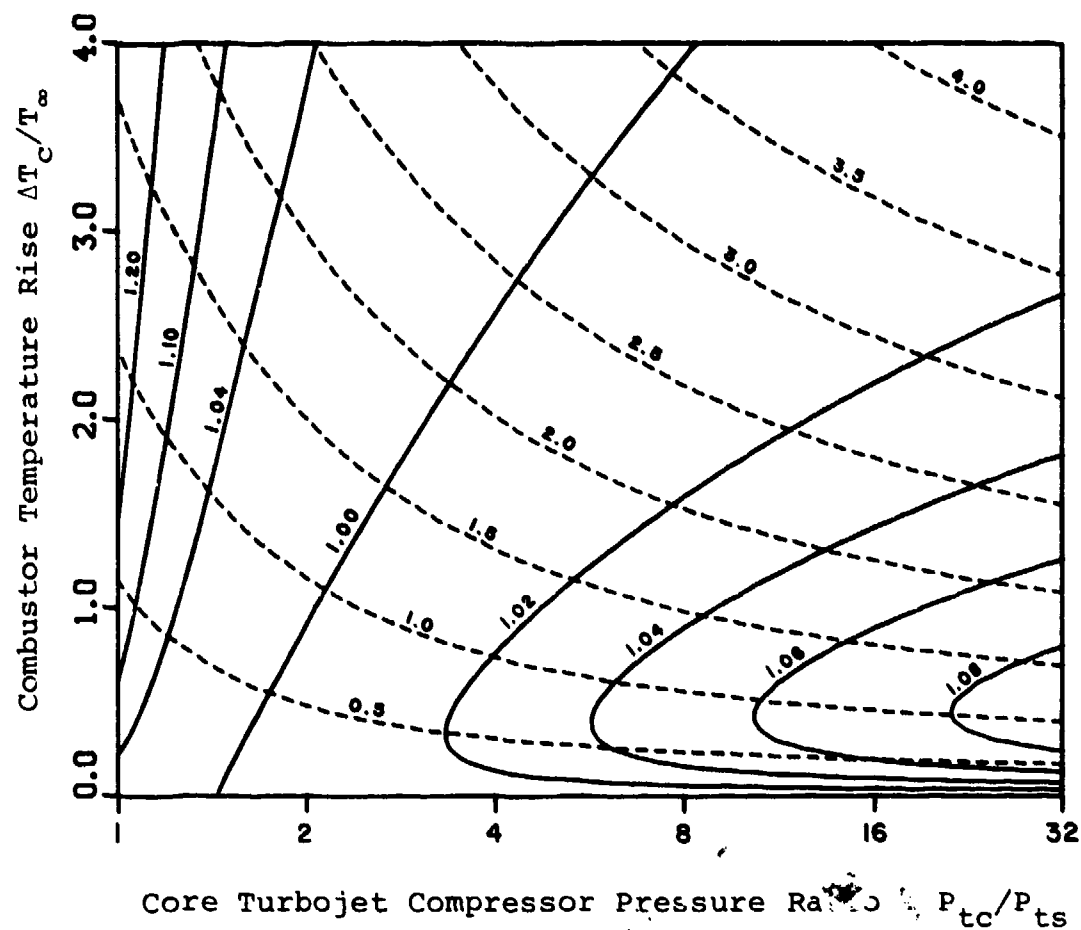


FIGURE 9 Performance Map for Ideal Ejectors with Turbine Engine Cores (Secondary/Primary Mass Flow Ratio $\beta = 5$)

b) Mach Number $M_\infty = 0.7$
 (—Augmentation Ratio ϕ , ---Specific Thrust f)

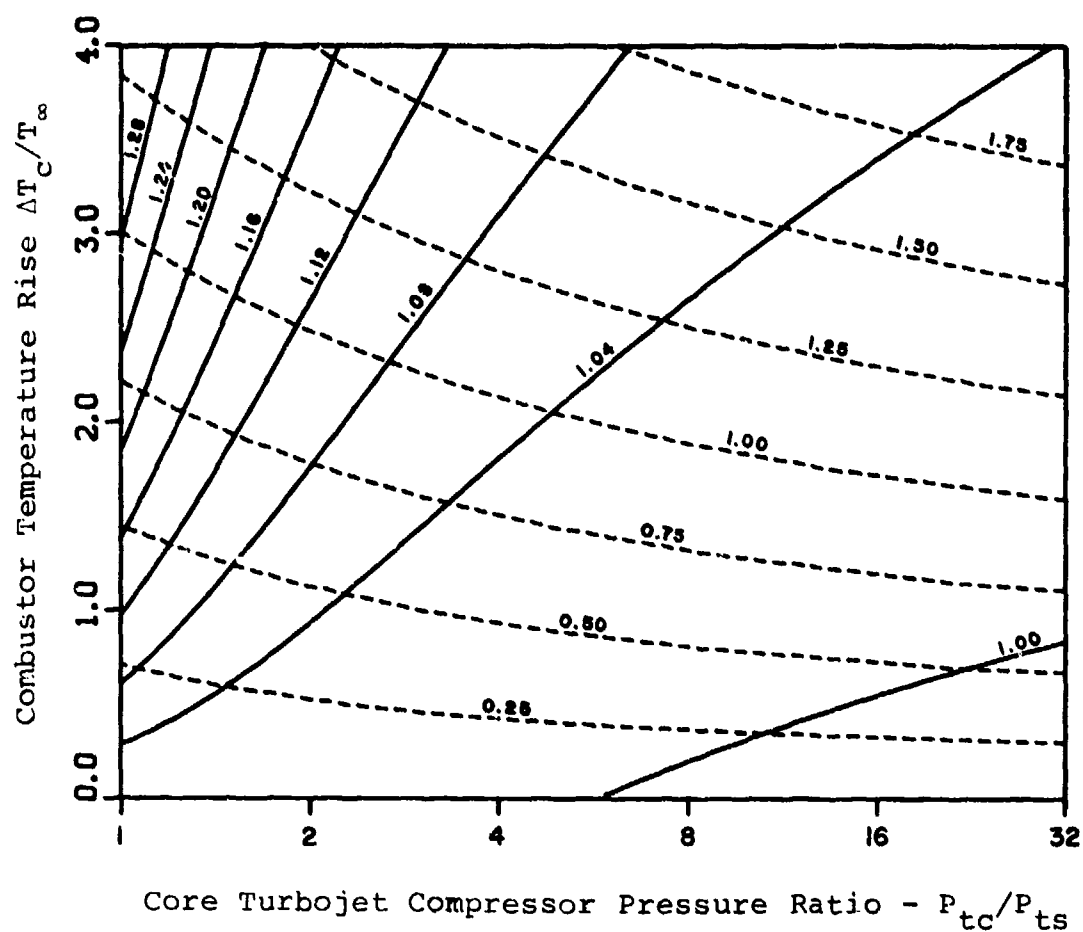


FIGURE 9 Performance Map for Ideal Ejectors with Turbine Engine Cores (Secondary/Primary Mass Flow Ratio $\beta = 5$)

c) Mach Number $M_\infty = 1.4$
 (—Augmentation Ratio ϕ , ---Specific Thrust f)

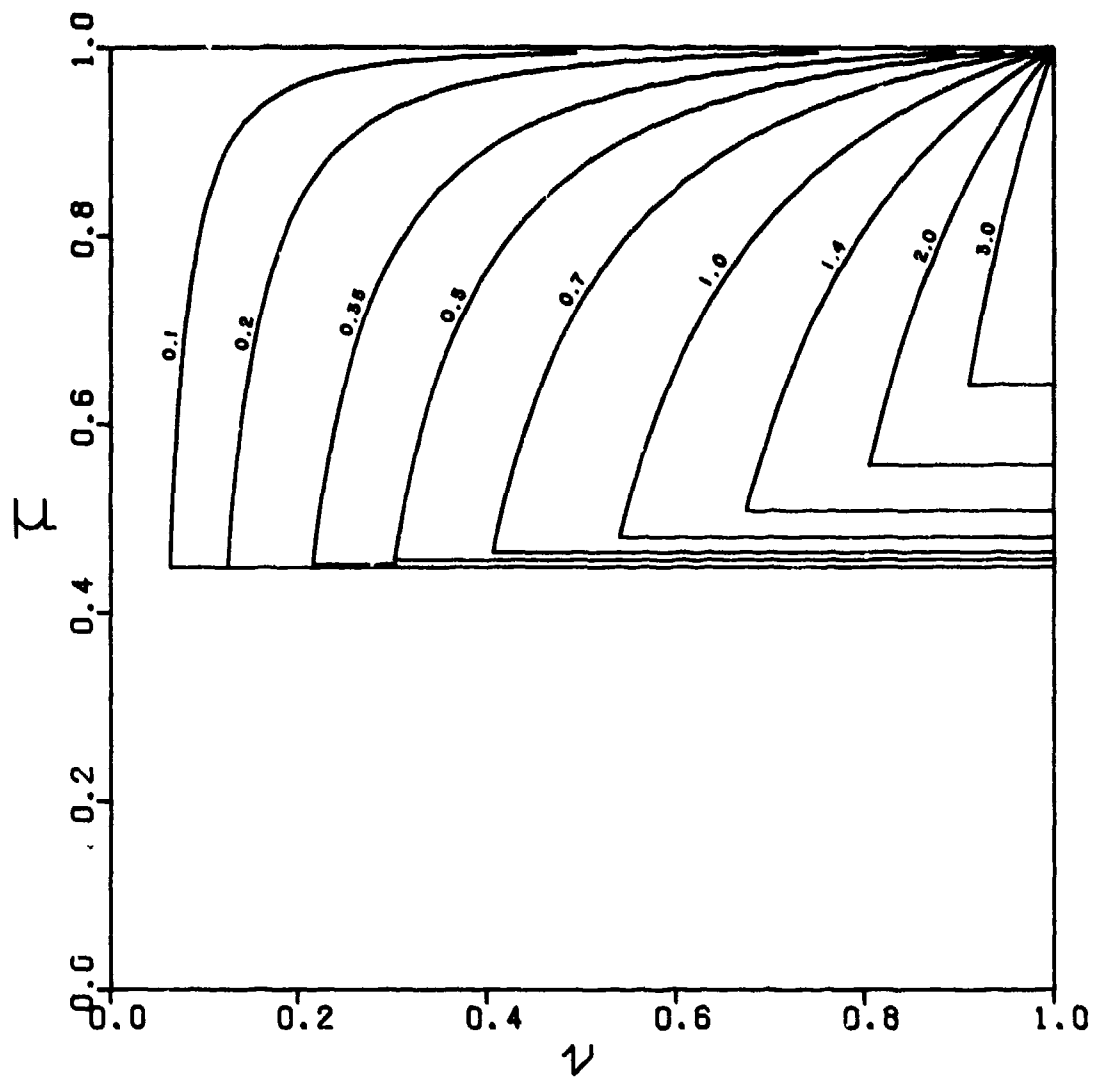


FIGURE 10 Mapping of the Core Turbine Engine of Figure 8 for Various Mach Numbers ($P_{tc}/P_{ts} = 1-32$, $\Delta T_c/T_\infty = 0-4$)

(The regions are to the right of the curves.)

REFERENCES

1. W. H. Heiser, "Thrust Augmentation," Journal of Engineering for Power (ASME Transactions), Vol 89, No 1, January 1967, pp 75-82.
2. R. M. Knox, "The Optimized Ejector-Nozzle Thrust Augmentor," Journal of the Aerospace Sciences, Vol 29, No 4, April 1962, pp. 470-471.
3. Equations, Tables and Charts for Compressible Flow, NACA Report 1135, 1953.
4. J. L. Porter, (Private Communication), August 1979.